# Brain Structural Covariance in Individuals at High Risk of Developing Psychosis: A Cross-Sectional and Longitudinal Study

Lucía de Hoyos González


Matthew Kempton

Department of Psychosis Studies
Institute of Psychiatry, Psychology and Neuroscience
King's College London
University of London

*Thesis in partial fulfilment for the degree of MSc in Neuroscience September, 2020.*

| *(Please tick)* | |
|---|---|
| **Research project involving data (Marking scheme 1)** | ✓ |
| **Literature review research project (Marking scheme 2)** | |
| **See Research Project Working Remote Handbook on pages on 10-11 for marking schemes.** | |

**Word Count**

| | | |
|---|---|---|
| Word Counts: | *Title*: | 16 |
| | *Abstract* (max 350): | 304 |
| | *Main Body* (not including Title, Abstract, References and Appendices; 7,500-10,000): | 8388 |

**Personal Statement**

I designed the project while I was working on my Bachelor Thesis at the *Instituto de Investigación Sanitaria Gregorio Marañón* in Madrid, Spain, with Dr Joost Janssen. However, this study differs from my Bachelor Thesis in the fact that my Bachelor Thesis had only a longitudinal design and this study has a cross-sectional design too. The data used belongs to the EU-GEI project (work package 5), in which the King's College is a part of.

The pre-processing of the images was carried out by Emily Hedges, who is currently doing her PhD with Dr Matthew Kempton. I performed the quality control of the images using the ENIGMA Cortical QC protocol. I also designed a new quality control (same-subject QC) to check if the images of the longitudinal dataset were correctly assigned to each subject (i.e. if the image 1 and image 2 of subject 1 had the same anatomical features and belonged indeed to subject 1). The obtention of the cortical thickness values was carried out by Emily Hedges.

As for the data analysis, this was carried out by me too (data correction, cross-sectional and longitudinal structural covariance, comparison of structural covariance matrices, FDR-correction, permutation control).

Dr Matthew Kempton provided support throughout this dissertation in our weekly meeting and checked the results obtained and the document produced.

## Abstract

Psychosis is a mental health condition with an early onset, which causes functional brain disruption and carries a great economic burden. Several neurological, psychiatric and medical disorders have symptoms of psychosis. However, its aetiology remains uncertain and usually has a poor response to treatment. Individuals at clinical-high risk (CHR) of developing psychosis can help disentangle the mechanisms behind the onset of psychosis. Brain structural alterations have been previously reported between controls and CHR subjects, and between CHR subjects who transition to psychosis (CHR-Ts) and those who do not (CHR-NTs). However, not all approaches have been successful in finding differences between groups. Structural covariance of cortical thickness has been related to developmental changes in anatomically connected brain regions (i.e. regions with a strong covariance belong to the same structural brain network). The objective of this study is to use new approaches to understand the mechanisms behind the risk of psychosis and its onset.

In this study, a cross-sectional and longitudinal approach of structural covariance with cortical thickness measures is used. The sample includes 297 subjects at baseline (65 controls, 232 CHR, 184 CHR-NTs and 48 CHR-Ts), 156 of which had also a follow-up scan (36 controls, 120 CHR, 96 CHR-NTs and 24 CHR-Ts).

Our results show differences between CHR-NTs and CHR-Ts in the cross-sectional (6 differences, FDR-corrected $p<.05$) and longitudinal (34 differences, FDR-corrected $p<.05$) analyses. In both, the frontotemporal regions were involved. In the case of controls and CHR subjects, only the longitudinal design showed significant differences (135 differences, FDR-corrected $p<.05$).

The importance of using new methods to analyse differences among groups is essential to study psychosis risk and onset. Further research on structural covariance networks of CHR subjects may help prevent and understand the transition to psychosis, expedite a more accurate treatment for those who develop psychosis and predict the development of the disorder.

# Table of contents


**CHAPTER 1. Introduction ..... 1**
Clinical High Risk ..... 1
Structural MRI in Clinical High Risk ..... 2
Cortical Thickness ..... 2
Structural Covariance ..... 3
Structural Covariance in CHR and psychosis ..... 5
EU-GEI study ..... 6
Motivation ..... 7
**CHAPTER 2. Materials and Methods ..... 8**
2.1. Sample ..... 8
2.2. Image Acquisition ..... 9
2.3. Image Processing ..... 10
2.3.1. Enigma Quality Control ..... 11
2.3.2. Same Subject Quality Control ..... 12
2.4. Structural Covariance Analysis ..... 14
2.4.1. Step 1: Data Selection ..... 15
2.4.2. Step 2: Extraction of Cortical Thickness Values ..... 15
2.4.3.1. Step 3, cross-sectional: Data Correction ..... 15
2.4.3.2. Step 3, longitudinal: Computation of Cortical Thickness Change ..... 16
2.4.3. Structural Covariance Matrices ..... 17
2.4.3.1. Significant Correlations ..... 18
2.4.3.2. Significant Differences ..... 18
**CHAPTER 3. Results ..... 20**
3.1. Sample Description ..... 20
3.1.1. Cross-sectional Sample ..... 20
3.1.2. Longitudinal Sample ..... 21
3.2. Cross-sectional Analysis ..... 21
3.3. Longitudinal Analysis ..... 25
**CHAPTER 4. Discussion ..... 30**
**References ..... 38**
**Appendix A. ComBat Results ..... 43**
**Appendix B: Cross-Sectional Analyses ..... 45**
**Appendix C. Longitudinal Analyses ..... 49**
**Appendix D. Region Abbreviations ..... 53**

# CHAPTER 1. Introduction

## Clinical High Risk

Psychosis is a mental health condition characterized by the loss of contact with reality and it is a symptom of some psychiatric and neurological conditions (for review see (1)). Its aetiology remains uncertain (2), but the scientific community supports that it entails an umbrella of genetic and environmental factors (2,3). Thus, research focuses on these to try to understand the risk of transitioning to psychosis and the onset of psychosis.

In the study of the transition to psychosis, the prodromal stages of psychosis (i.e. early signs and symptoms) have been established. Those subjects who have subclinical symptoms (e.g. hallucinations or delusions) but have not transitioned to psychosis yet, are known as clinical high risk (CHR) subjects (4). Other acronyms for these are ARMS (at-risk mental state) and UHR (ultra-high risk). These individuals have a heightened risk for developing psychosis due to belonging to the vulnerability group (genetic risk factor for psychosis due to first-degree relative with psychosis or the subject having a schizotypal personality disorder), to the attenuated psychosis group or to the BLIPs (brief limited intermittent psychotic symptoms) group. Moreover, these subjects present some deficits at the cognitive and social levels (5,6). Even though these subjects are at high risk of developing psychosis, the transition is not inevitable, which suggests that other mechanisms may be involved (4). Fusar-Poli et al. stated the approximate rates of transition to psychosis at 22% after a year, 29% after two years and 36% after three years (7). Both, the characterization of CHR subjects and the establishment of these other mechanisms, are highly important at the clinical level for an early intervention and in order to prevent these subjects from transitioning to psychosis (8,9).

## Structural MRI in Clinical High Risk

Brain structural alterations in schizophrenia and related psychosis have been reported. Research has focused on the changes in grey matter tissue, hypothesizing that such change is related to schizophrenia or is a predictor of its onset (10). A loss of grey matter tissue has been reported in first-episode and chronic schizophrenia subjects (11) and the onset of psychosis has been associated to progressive brain structural alterations (12-14). Moreover, there is evidence that shows a gradual loss of brain tissue related to the first psychotic episode in schizophrenia patients, especially in prefrontal and temporal lobes (15), yet the direction of causality remains unclear due to the difficulty of distinguishing between pathological and developmental changes in brain structure during adolescence (16).

As an attempt to throw light upon whether the structural changes are caused by the transition to psychosis or as a consequence of it, studies have focused on the structural brain differences between CHR 'converters' (CHR-Ts) and CHR 'non-converters' (CHR-NTs). The findings from two of this type of studies (12,15), both with a longitudinal design, suggested a greater tissue loss in CHR individuals. However, due to a lack of statistical power, neither of these could find significant differences in the rates of tissue loss between CHR-Ts and CHR-NTs. Despite this, longitudinal designs have been suggested to better establish differences between these two subgroups, as the effect of the onset of psychosis can be studied in more detail (13).

## Cortical Thickness

With special regards to the biomarker that will be used in this study, cortical thickness, the structural alterations mentioned above also encompass alterations in cortical thickness of CHR patients (17,18). Cortical thickness, or CT, measures the

amount of grey matter between cortical layers (Figure 1). The relation between cortical thickness, brain development and brain disorders has been previously reported (19). Thus, it is a biomarker which is widely used in neuroimaging and psychiatric research. Studies have reported cortical thinning in CHR subjects, where those who finally transition to psychosis show a greater loss of cortical thickness (17).

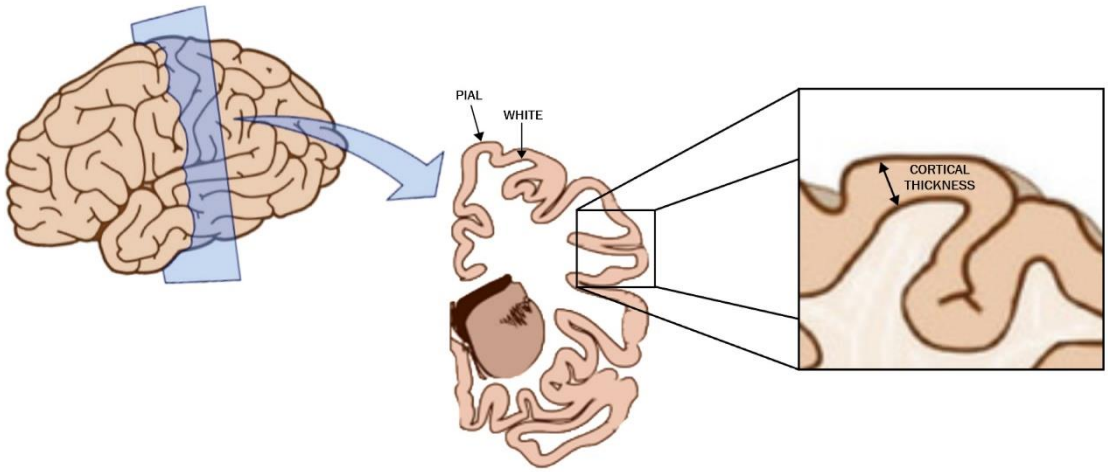


**Figure 1. Cortical Thickness (CT).** It is the biomarker used in this study and it is obtained by measuring the distance between the white and pial surfaces, obtaining the amount of grey matter between these layers.

## Structural Covariance

The findings from voxel-based morphometry studies and region-of-interest studies centre on focal regions rather than networks. However, previous literature supports that brain structural alterations in schizophrenia and related psychosis are distributed via brain networks (20). Thus, understanding the brain as a network may help elucidate the onset of psychosis in CHR subjects. In order to study the brain connectivity patterns, the method of structural covariance can be used.

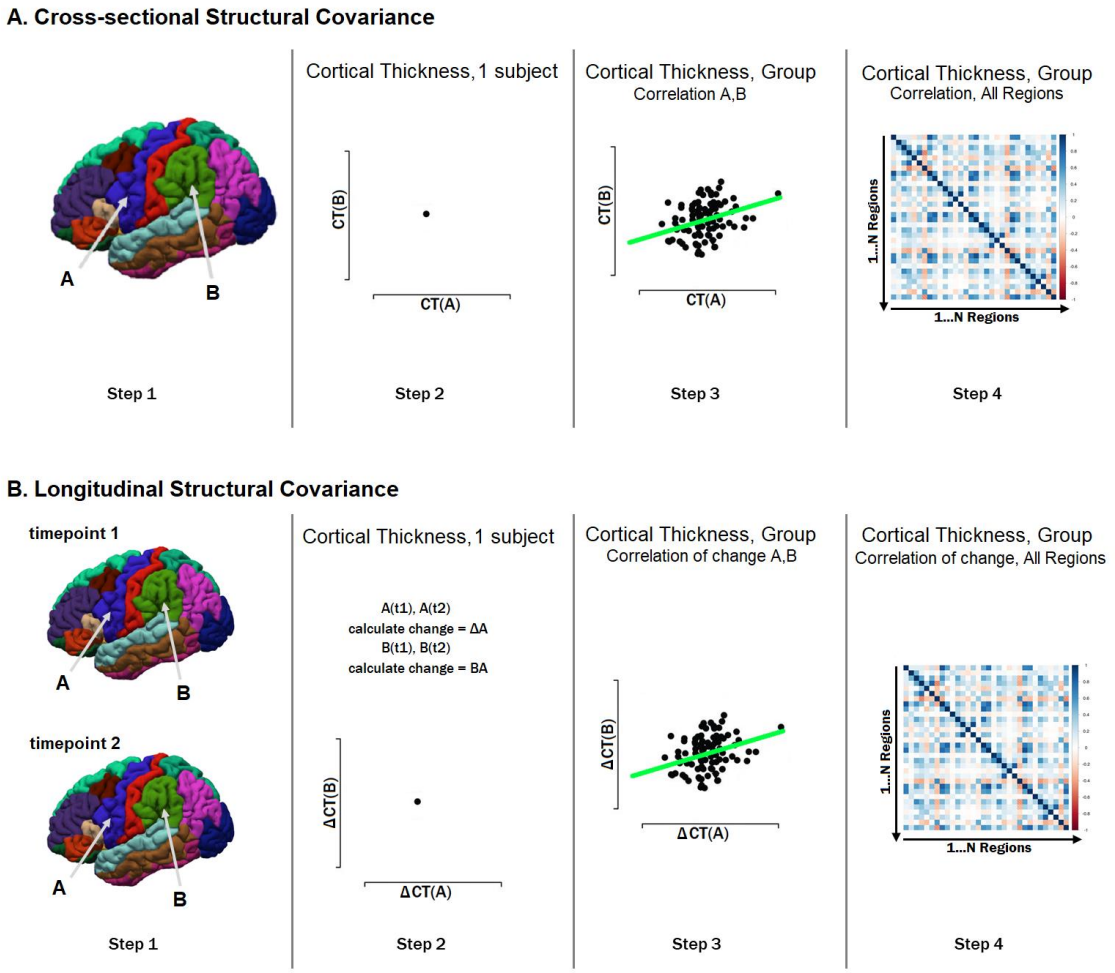


**Figure 2. Computation of structural covariance group matrix. (A) Cross-sectional design.** Step 1: Take two regions A and B. Step 2: Obtain the cortical thickness values of one subject and put them on a plot where each axis represents the cortical thickness of a region (e.g. x-axis CT(A), y-axis CT(B)). Step 3: Repeat step 2 for all the subjects in the group and obtain the fitted line (its slope is the correlation value ($r^2$) between both regions for the group). Step 4: Repeat steps 1 to 3 for all the pairs of regions and obtain the structural covariance group-matrix. **(B) Longitudinal design.** Step 1: Take two regions A and B from the same subject at two different timepoints. Step 2: Compute the change in cortical thickness of regions A and B (ΔCT(A), ΔCT(B)) for that subject and put the obtained values on a plot where each axis represents the change in cortical thickness of a region (e.g. x-axis ΔCT(A), y-axis ΔCT(B)). Step 3: Repeat step 2 for all the subjects in the group and obtain the fitted line (its slope is the correlation value ($r^2$) between both regions for the group). Step 4: Repeat steps 1 to 3 for all the pairs of regions and obtain the structural covariance group-matrix.

Structural covariance studies the similarity in developmental trajectories of two or more brain regions using biomarkers (Figure 2A), such as, cortical thickness (21). Alexander-Bloch et al. proved the relationship between structural brain

networks and functional brain networks using structural covariance matrices of cortical thickness (21). Thus, suggesting that brain regions which tend to covary belong to the same brain network. Furthermore, neuroimaging studies using diffusion tensor imaging and functional MRI have reported an increase in functional connectivity between regions showing high structural covariance (22-24). Structural covariance offers a great opportunity to examine the changes in the brain network development. Structural covariance networks are also influenced and regulated by genetic factors (25), nevertheless, other factors such as environmental factors are said to also influence the structural covariance patterns in the brain (25,26). In view of this, structural covariance is a powerful approach to study the effects of genetic and environmental factors on brain development and onset of psychosis.

To further study the covariance between brain regions, structural covariance can also be studied with a longitudinal design (Figure 2B). This is, the covariance of (e.g. cortical thickness) change (i.e. synchronized change) between brain regions can be reported. By doing so, the brain developmental processes that may be involved in the transition to psychosis can be studied. Many studies have reported maturational structural covariance networks in the healthy and diseased brain (21).

### Structural Covariance in CHR and psychosis

Structural covariance of brain regions that belong to key networks is known to change along normal development and with age (27,28). However, a difference in the patterns of change in structural covariance has been reported in CHR subjects (10). It has been recently reported a higher structural covariance between regions in the right prefrontal cortex in CHR patients (29). Also, longitudinal studies show a greater contraction of the prefrontal region in CHR-Ts subjects (13). All these findings may suggest that as well as the differences in grey matter measures (e.g. cortical

thickness) that have been reported in CHR subject before onset, there are structural covariance patterns which may be psychosis-related (29).

Moreover, there are some findings regarding structural covariance on schizophrenia and first-episode psychosis patients. Regarding the comparison between healthy controls and schizophrenia, the regions of pars orbitalis and insula had a higher relationship (integrity-closeness) between them and with other brain regions in schizophrenia patients (30). However, such study, which combined structural covariance with graph theory, found no significant differences between schizophrenia and first-episode psychosis subjects. Another study, which compared schizophrenia patients that responded to treatment to the ones that did not, detected higher structural covariance within the executive network at baseline in the former group was associated to better response to treatment after two years (31). Thus, suggesting that by studying structural covariance at the network level, the outcome to treatment response could be predicted. In view of this, by using this approach to study the integrity of structural networks in healthy controls, CHR-Ts and CHR-NTs, it may be possible to understand the difference between healthy controls and people at CHR, and to try to differentiate between the structural networks of CHR-Ts and CHR-NTs and maybe use this as a predictor of the transition to psychosis.

### EU-GEI study

The European Network of National Schizophrenia Networks Studying Gene-Environment Interactions (EU-GEI) is a multi-site and international (more than 15 countries) study. It focuses on the gene-environment interaction of schizophrenia subjects and it has clinical, neuroimaging, genetic, phenotypic and environmental data (32). Within this study, there are also CHR subjects, including subjects that transition to psychosis. Thus, the sample from the EU-GEI study is valuable for this study.

## Motivation

After all of the above has been mentioned, there is a need to continue studying the differences between healthy controls and CHR subjects, but, above that, it is even more important to understand the difference between CHR-Ts and CHR-NTs to try to uncover the mechanisms behind the onset of psychosis. Many studies have tried to divide these last two groups by looking at the brain as an entity composed by different regions, rather than as an inter-connected network where regions influence and interact with one another. Thus, the method of structural covariance allows this perspective of the brain. There have been a small number of studies analysing structural covariance in CHR. By looking at the covariance between regions (cross-sectional design) as well as the covariance of change of brain regions (longitudinal design), with a large sample size, the aim is to understand the difference in brain structure and brain maturational networks between healthy controls and CHR subjects and between CHR-Ts and CHR-NTs.

# CHAPTER 2. Materials and Methods

## 2.1. Sample

The sample used corresponds to a large, multi-site longitudinal sample with T1-weighted magnetic resonance images obtained between the July 2010 and August 2016, through an international collaboration with the EU-GEI project, being King's College London one of the collaborating sites.

The inclusion criteria for the CHR subjects was based on the Comprehensive Assessment of At-Risk Mental States (CAARMS) (33). CAARMS psychosis threshold criteria were also used to assess the transition or no transition to psychosis after baseline, followed by the confirmation of a clinical interview following the DSM-IV Axis I Disorders (34). The subjects met the research diagnostic criteria of not having any present or past psychotic or neurological disorders, substance abuse or dependence (DSM-IV criteria) and an IQ above 60. Antipsychotic exposure was not an exclusion criterion only if it was not prescribed for a psychotic event. As for the healthy controls, exclusion criteria were having a previous psychotic episode determined by the SCID, an IQ below 60 and having previous antipsychotic exposure. Healthy controls could not meet the inclusion criteria for CHR subjects. For every subject age at scan, sex, ethnicity and years of education were reported from the Medical Research Council Sociodemographic Schedule (35). The control group aimed to match the CHR group by age, gender and ethnicity -ordered by priority-. Also, for all participants, 3-Tesla magnetic resonance images were taken.

From the initial dataset (n=411 subject), for the cross-sectional analysis, a subset with 297 unique subjects were included (232 CHR subjects and 65 healthy controls), all of whom had a baseline scan. As for the longitudinal analysis, only those subjects with a baseline scan and at least 2 scans were included and scanned at the

same scanner (137 CHR subjects and 36 healthy controls). Exclusion of subjects due to quality assurance procedures is described below, in the image processing section.

## 2.2. Image Acquisition

The neuroimaging data was obtained from nine different psychosis early detection sites. All sites used the ADNI-2 T1 acquisition protocol (http://adni.loni.usc.edu/methods/documents/mri-protocols/). The scanners used to obtain the images changed from one site to another (see Table 1). Regarding the scanners of the Netherlands, subjects recruited in Amsterdam and The Hague were both scanned in Amsterdam. However, in Amsterdam the scanner changed to a newer scanner during the project (in Table 1 scanners 2 and 3 both belong to the same site due to this change).

**Table 1. Scanners used for image acquisition and site.**

| ID | Scanner | Site |
|---|---|---|
| *1* | 3T GE SIGNA HDx | London, United Kingdom |
| *2* | 3T Philips Intera | Amsterdam, Netherlands |
| *3* | 3T Philips Ingenia | Amsterdam, Netherlands |
| *4* | 3T Siemens MAGNETOM TrioTim | Vienna, Austria |
| *5* | 3T Siemens MAGNETOM Verio | Basel, Switzerland |
| *6* | 3T Siemens MAGNETOM TrioTim | Cologne, Germany |
| *7* | 3T Siemens MAGNETOM TrioTim | Melbourne, Australia |
| *8* | 3T Philips Achieva | Copenhagen, Denmark |
| *9* | 3T Siemens MAGNETOM TrioTim | Paris, France |

## 2.3. Image Processing

In order to obtain the values of cortical thickness from each scan, after the images are acquired, they have to be processed. Currently, automatized techniques are used to process the images. Surface-based morphometry (SBM) is one of these techniques and is the one used within this study. To do so, FreeSurfer was used to analyse and process the T1-weighted MRI images. The pipeline that this software uses can be seen in Figure 3. After the surface extraction step, the cortical thickness values are measured at each region of interest. The regions of interest will depend on the brain parcellation system used. In this study, the Desikan-Killiany atlas (36) was used.

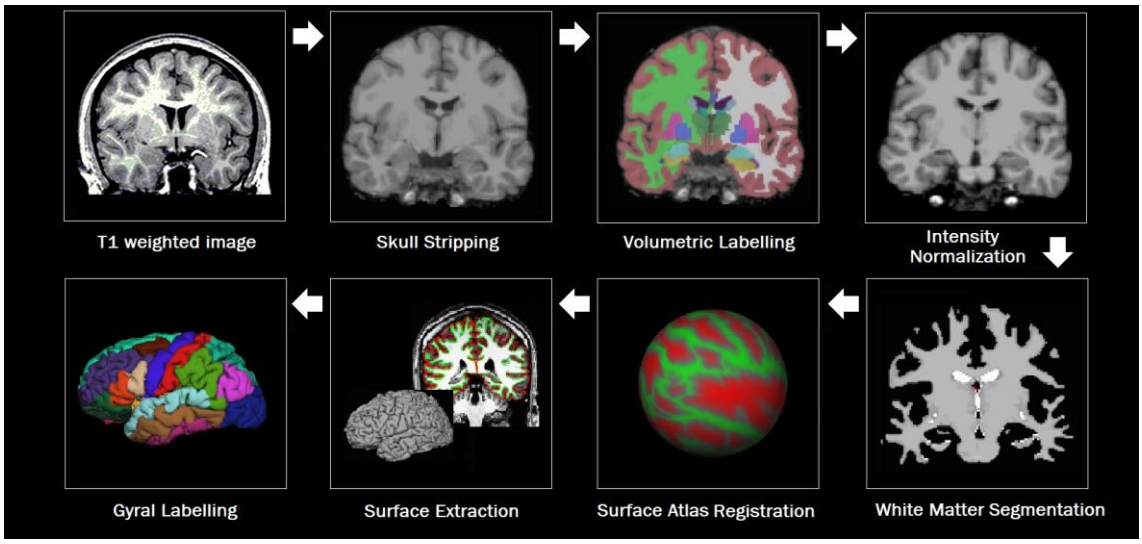


**Figure 3. FreeSurfer pipeline.** The pre-processing pipeline of FreeSurfer consists of eight steps. First, obtain the T1 weighted image from the subject. Then, the skull is removed to keep only the brain. After that, the different brain tissues and volumes are labelled (e.g. white matter, grey matter, etc). Then, based on the volumetric labelling, there is an intensity normalisation to generate higher contrast between tissues. After this, the white matter tissue is isolated. Then, the next two steps start working on surfaces. First, there is the atlas registration and then surface extraction (e.g. pial and white surfaces). Finally, based on the brain atlas selected, the brain is parcellated into regions of interest. Now the images have been pre-processed and need to undergo quality control procedures to ensure that this pipeline has not encountered any problems.

### *2.3.1. Enigma Quality Control*

Once the images were processed with FreeSurfer, in order to ensure their correct processing, they must undergo quality control (QC) procedures. The QC ran in this project was the enigma cortical QC protocol (http://enigma.ini.usc.edu/protocols/imaging-protocols/). The enigma QC consists of three quality checks: outlier detection, internal quality control and external quality control.

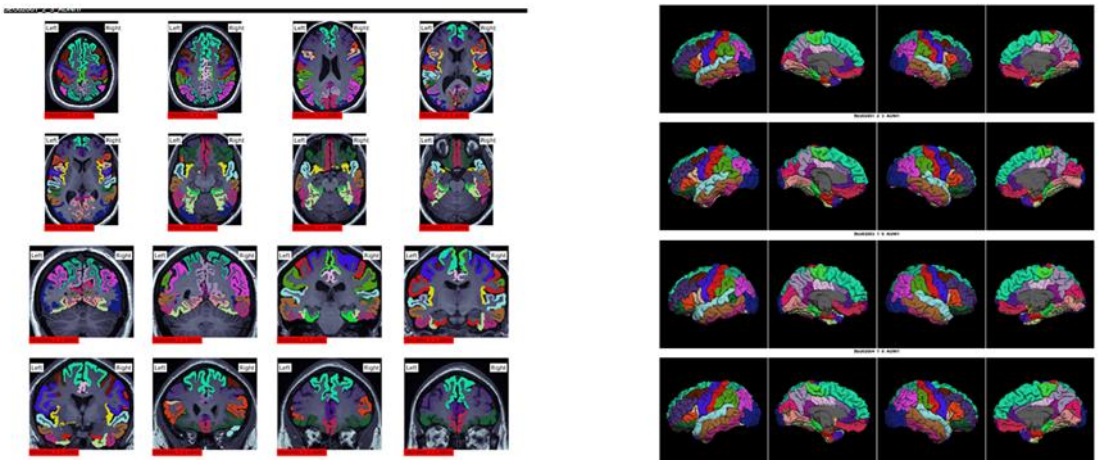

**Figure 4. Internal (left) and External (right) quality control using the ENIGMA protocol.**

For the outlier detection, two different datasets were used: all the scans included in the dataset (n=623 scans) and only baseline scans (n=297 scans). This step extracts the mean cortical thickness and the mean surface area of each region of interest for each subjects and searches for the outliers. The protocol outputs the subject IDs of those subjects that have higher or lower values of either cortical thickness or surface area. As for the internal and external QC, the images produced by the protocol (Figure 4) had to be manually checked. The manual check consists of looking at all subjects and checking that the borders of the regions of interest have been correctly assigned. In the case of the Desikan-Killiany atlas, it is based on a gyral parcellation, thus, usually regions finish at a certain gyrus. Common mislabels

detected during the QC were, overestimation of the banks superior temporal sulcus region and the meninges (see Figure 5).

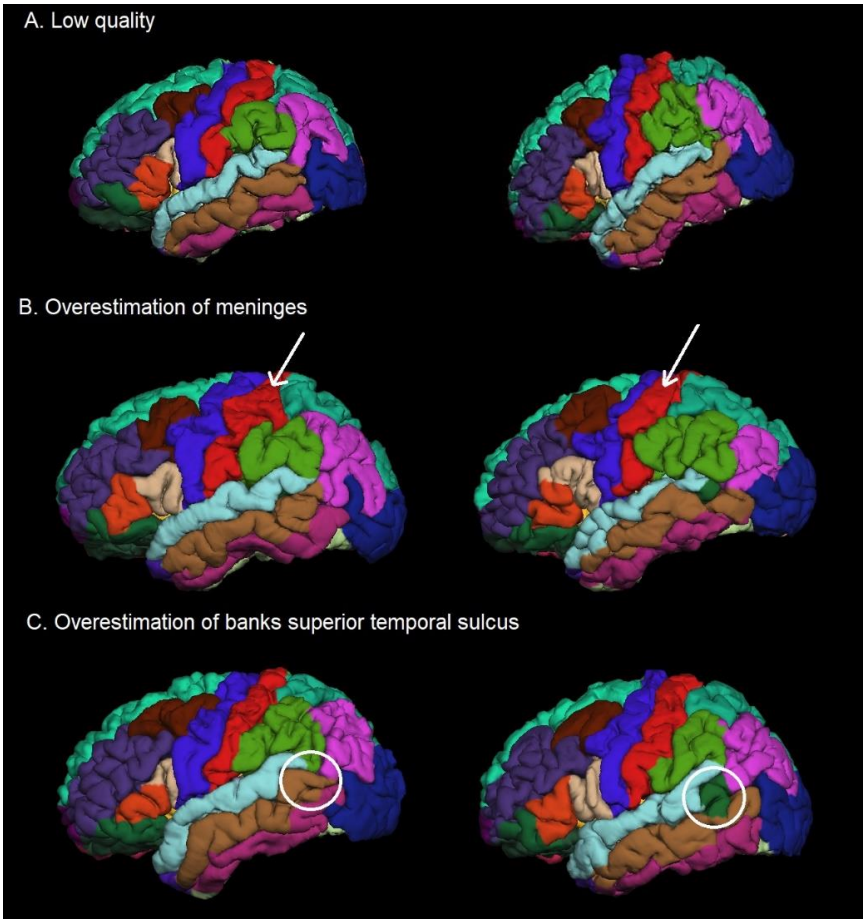


**Figure 5. Common mislabels.** (A) Low quality (right) compared to normal quality (left). (B) Overestimation of meninges (arrow). (C) Overestimation of banks superior temporal sulcus of the right image (green region inside the circle) compared to the left image.

### *2.3.2. Same Subject Quality Control*

In order to reassure the longitudinal images of the sample were correctly assigned to each subject, I designed a new QC protocol named 'same-subject quality control' for this purpose. The code to run such QC is available at github.com/ldehoyos/ssQC. At this GitHub there is a manual that explains in more detail the QC. Briefly, the same-subject QC consists of 4 steps:

1. Extract the orig.mgz files for each subject. This is the output file from FreeSurfer which will be used to obtain the PNG image in the next step.

2. Create a PNG image of the sagittal view of each subject. To create the PNG image, the program selects the middle image between the two side slices. The side slices are the slices at each side of the head of the patient (see Figure 6). This is useful, because if a pre-set slice was always selected (e.g. slice 125), the view obtained will not be the same among all images (as the absolute position of the subjects changes from one scan to another, they are not always centred in the image). Using the side slices, the final output obtained is more homogeneous (usually the most medial view).

3. Order the images and sort them into subject folders. A folder is created for each subject. Within that folder the images from all the subject's timepoints are placed. The timepoints will be named as ADNI followed by the timepoint number (e.g. ADNI1).

4. Display the images in a html file to visualize the results and detect any possible mislabels. In this file, each row is a subject and each column a timepoint.

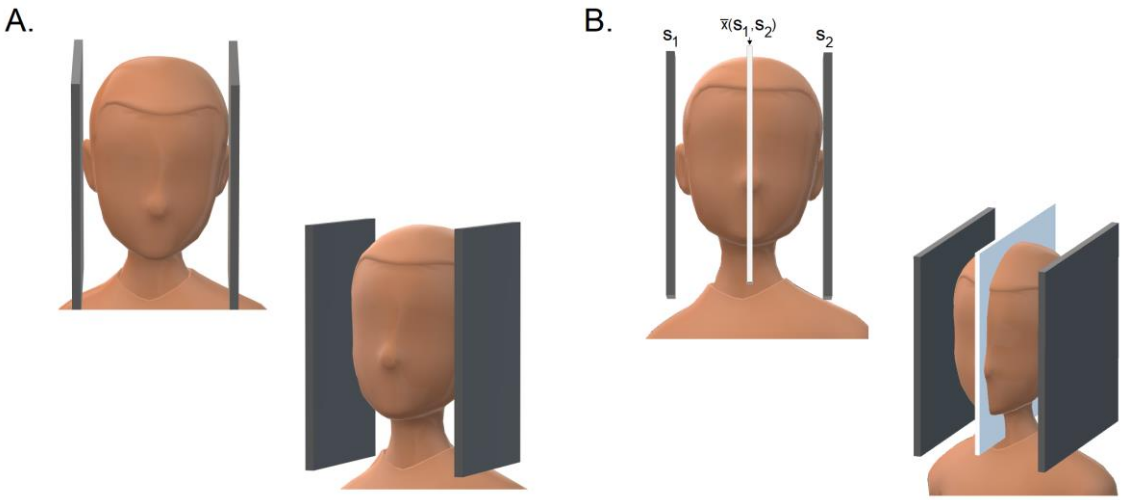


**Figure 6. Side slices**. (A) Side slices in grey. These slices are the ones at each side of the head of the subject. (B) Side slices and mean slice (white). The mean slice is the one selected to output the sagittal image in the same-subject QC.

## 2.4. Structural Covariance Analysis

The data was analysed using a pipeline created in R (www.r-project.org), which is an open source programming language widely used to run statistical analysis. The workflow of this analysis can be seen in Figure 7 and will be explained within this section.

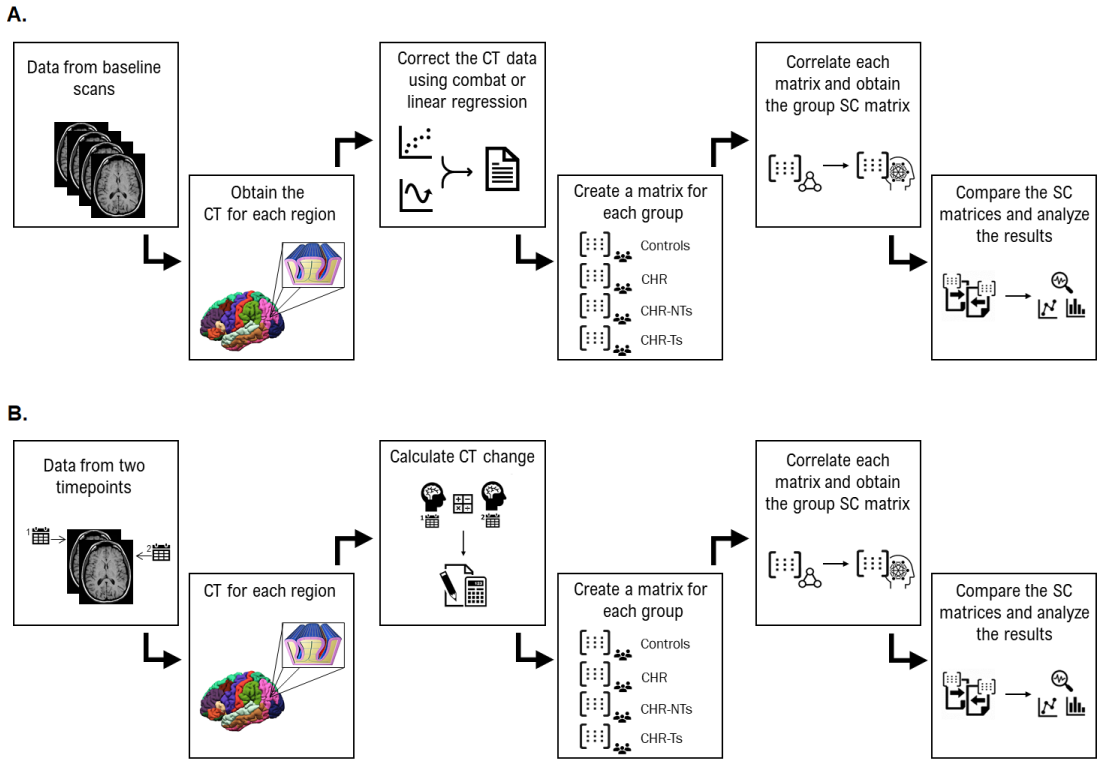


**Figure 7. Workflow of the structural covariance analysis of (A) baseline images and (B) longitudinal images.** First the data is collected: baseline images for cross-sectional and baseline and follow-up images for longitudinal. Then, for each image, the cortical thickness (CT) values are extracted from the 68 regions of interest of the Desikan-Killiany atlas. After that, the data either undergoes correction (linear regression and comBat), for the cross-sectional analysis, or the change of cortical thickness is computed, for the longitudinal analysis. Then, a matrix for each group (controls, CHR, CHR-NTs and CHR-Ts) is created. Once this is done, each of those matrices is correlated using Pearson's r to obtain the structural covariance (SC) matrices. Finally, the matrices are compared (see Figure 6 for more detail) and the results are analysed. Abbreviations: clinical high-risk (CHR), clinical high-risk transitioned (CHR-Ts) and clinical high-risk no transition (CHR-NTs).

### 2.4.1. Step 1: Data Selection

The structural covariance analysis carried out in this study consists of two different analysis: cross-sectional and longitudinal. For the cross-sectional analysis, all the baseline scans which passed the QC procedures, were included. As for the longitudinal analysis, the inclusion criteria establish that the subject has a baseline scan and a second scan (both must have passed the QC).

### 2.4.2. Step 2: Extraction of Cortical Thickness Values

The images have been pre-processed with FreeSurfer, using the Desikan-Killiany atlas (36), which has 68 regions of interest (Figure 8). Then, the images went through the QC procedures. For the structural covariance analysis, the mean cortical thickness values of each brain region of the scans that passed the QC were extracted.

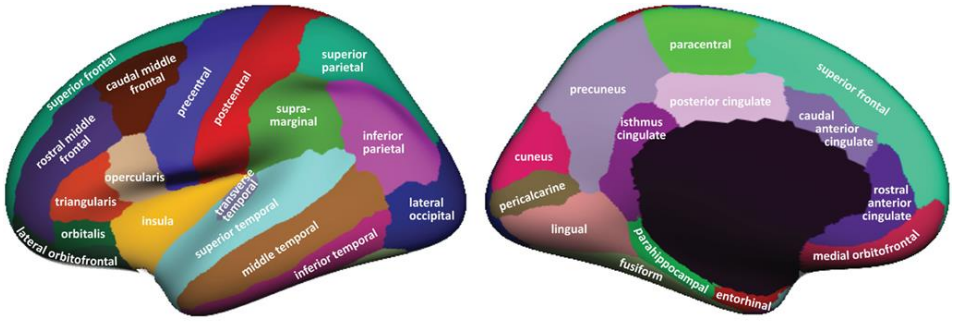


**Figure 8. Lateral (left) and medial (right) view of the regions of interest in the Desikan-Killiany atlas.** Each region is displayed in a different colour and its name is written within the region. This image only displays the regions of one hemisphere (34) but the same parcellation system is used for both hemispheres.

### 2.4.3.1. Step 3, cross-sectional: Data Correction

For the cross-sectional analysis, the cortical thickness data was corrected for the covariates which had a significant effect over mean cortical thickness (left and right hemisphere). These are age ($p_{left}$<2.20e-16; $p_{right}$=7.98e-16), sex ($p_{left}$=0.63;

$p_{right}$=0.57), scanner ($p_{left}$=2.94e-10; $p_{right}$=2.70e-08) and ethnicity ($p_{left}$=9.13e-03; $p_{right}$=2.53e-02). Even though, sex does not have a significant effect over cortical thickness, it was included as a covariate due to the previously reported sex-differences in cortical thickness (37,38). Nevertheless, the proportion of females and males in each group was almost 50:50 (see Tables 2 and 3 in results). To carry out the data correction, two different corrections were used: linear regression and ComBat (39).

Linear regression is a commonly used method to remove confounder effects (40). In this study, the covariates used were age, sex, scanner and ethnicity. To do so, dummy coding of the scanner (9 values) and ethnicity (6 values) variables was used. Then, for the structural covariance analysis, the residuals were used.

As for the ComBat correction, this method is an empirical Bayes method developed to correct genomics data (41), but posterior studies implemented this method in neuroimaging data (39). ComBat has been proven very useful for multi-site data, which is often scanned in different scanners. This method has been implemented using the GitHub from Fortin et al. (https://github.com/Jfortin1/ComBatHarmonization). The data was corrected for the same covariates as the linear regression. For the structural covariance, the corrected values (the output of ComBat function) were used. Due to the similarity of results between the data corrected with linear regression or ComBat, the results obtained from the values corrected with ComBat can be seen in Appendix A.

#### *2.4.3.2. Step 3, longitudinal: Computation of Cortical Thickness Change*

For the longitudinal analysis, the data was not corrected using neither of the aforementioned methods. In this case, the formula used to calculate the value of cortical thickness change takes into consideration the possible confounders (age and

brain size - which involves sex and ethnicity-). Brain size is related to sex (males have, on average, larger absolute brain size compared to females (42-44)) and ethnicity (45). The formula accounts for brain size by dividing the difference between cortical thickness values by the mean of both values (see Equation 1). Age is accounted for by dividing by the time between scans. Furthermore, the change of cortical thickness is weighted by the mean cortical thickness over time, thus, it removes the possible bias of cortical thickness change caused by larger or smaller cortical thickness values (i.e. a thicker cortex has larger change of cortical thickness (46)). As for scanner, only those subjects who were scanned in the same scanner in both timepoints, were included.

The annual percentual change (APC) is the formula used to compute the value of cortical thickness change (Equation 1). APC is calculated as the difference between the cortical thickness at the second timepoint minus the cortical thickness at the first timepoint, all of that divided by the mean of both values, which is in turn divided by the time between scans in years. Finally, to convert the value to percentage, this quotient is multiplied by a hundred.

$$APC = \frac{\frac{CT_{timepoint2} - CT_{timepoint1}}{mean\left(CT_{timepoint1}, CT_{timepoint2}\right)}}{time\ between\ scans\ in\ years} * 100$$

**Equation 1. Annual Percentual Change Computation.**

### *2.4.3. Structural Covariance Matrices*

Once the data had been prepared, either corrected or converted to APC, it was divided into four groups: healthy controls (cross-sectional n=65, longitudinal

n=36), CHR (cross-sectional n=135, longitudinal n=136), CHR no transition (cross-sectional n=184, longitudinal n=108) and CHR transition (cross-sectional n=48, longitudinal n=28). Note that even though the CHR subjects were initially 232, in the analysis of differences between controls and CHR subjects only 135 CHR subjects were included. These were those subjects that had been scanned at the same sites as the controls (i.e. scanners 1, 3 and 7). This was done to avoid a possible scanner bias. Structural covariance matrices were created by correlating the data of each group using Pearson's correlation, thus having 2278 unique correlations in each matrix (Equation 2).

$$Number\ of\ unique\ correlations = {nROI\ x\ (nROI - 1)}/{2}$$

**Equation 2. Number of unique correlations.** It is computed as the number of regions of interest (nROI) multiplied by the same value minus one. Then, that product is divided by two (as the correlation matrix is symmetric).

### *2.4.3.1. Significant Correlations*

To establish the significant correlations of each group, permutation testing was used (n=100,000). In each permutation, the subjects were randomly assigned to one group or another, and then, the data was correlated to obtain the structural covariance matrices. To calculate the p-value for each correlation, its real value was compared to the random distribution.

### *2.4.3.2. Significant Differences*

To compare the matrices, two different comparisons were made: healthy controls vs CHR and CHR-NTs vs CHR-Ts. For the first comparison, in the cross-

sectional analysis, only the CHR that were scanned with the same scanners as the healthy controls were selected to avoid possible confounding effects. This was not applied to the longitudinal analysis in order to try to keep the sample size as larger as possible.

For each comparison (see Figure 9), the structural covariance matrices were converted to Fisher-Z. Then, the z-observed of the difference matrix was computed. For the first comparison, the difference matrix was calculated as the healthy controls' Z-matrix squared minus the CHR' Z-matrix squared. For the second comparison, the difference matrix was computed by subtracting the CHR-NTs Z-matrix squared to the CHR-Ts Z-matrix squared.

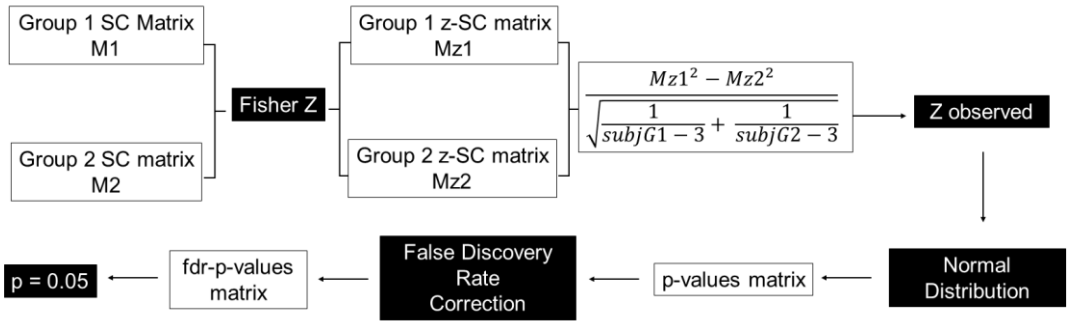


**Figure 9. Comparison of structural covariance (SC) matrices.** The structural covariance matrices of the two groups (M1, M2) are converted to Fisher Z (M1 to $Mz_1$, M2 to $Mz_2$). Then, the Z-observed of the difference matrix ($Mz_1^2$-$Mz_2^2$) is computed by dividing the matrix by the square root of: one divided by the number of subjects from group 1 (subjG1) minus 3, plus one divided by the number of subjects from group 2 (subjG2) minus 3. Then, the values are normally distributed, obtaining the matrix of p-values. Due to multiple comparisons, a correction is needed, thus, the false discovery rate (FDR) correction is applied. Then, to the matrix of fdr-corrected p values, a threshold of p=0.05 is applied.

# CHAPTER 3. Results

## 3.1. Sample Description

### *3.1.1. Cross-sectional Sample*

**Table 2. Description of the Cross-sectional Sample.** The table shows the descriptives of age, sex, scanner and ethnicity for each group used in the analysis: Controls, CHR (all the subjects -ALL- and only those who were scanned at the same centres as the controls -analysed-, the latter one was the sample used in the analysis), CHR-NTs and CHR-Ts. Abbreviations: clinical high risk (CHR), no transition (NTs) and transition (Ts).

| | Controls | CHR | | CHR-NTs | CHR-Ts |
|---|---|---|---|---|---|
| | | *ALL* | *Filter* | | |
| **n Subjects** | 65 | 232 | 135 | 184 | 48 |
| **Age** | 22.95 (4.11) | 22.47 (4.48) | 22.07 (4.59) | 22.59 (4.54) | 21.98 (4.24) |
| **Male** | 34 | 120 | 66 | 93 | 27 |
| **Female** | 31 | 112 | 69 | 91 | 21 |
| ***Scanner*** | | | | | |
| 1 | 38 | 68 | 68 | 52 | 16 |
| 2 | - | 28 | - | 25 | 3 |
| 3 | 9 | 37 | 37 | 36 | 1 |
| 4 | - | 7 | - | 4 | 3 |
| 5 | - | 20 | - | 16 | 4 |
| 6 | - | 7 | - | 3 | 4 |
| 7 | 18 | 30 | 30 | 24 | 6 |
| 8 | - | 16 | - | 12 | 4 |
| 9 | - | 19 | - | 12 | 7 |
| ***Ethnicity*** | | | | | |
| White | 42 | 167 | 88 | 133 | 34 |
| Black | 10 | 22 | 18 | 15 | 7 |
| Mixed | 5 | 20 | 12 | 17 | 3 |
| Asian | 8 | 5 | 4 | 4 | 1 |
| North African | - | 10 | 6 | 8 | 2 |
| Other | - | 8 | 7 | 7 | 1 |

### *3.1.2. Longitudinal Sample*

**Table 3. Description of the Longitudinal Sample.** The table shows the descriptives of age, sex, scanner and ethnicity for each group used in the analysis: Controls, CHR, CHR-NTs and CHR-Ts. Abbreviations: clinical high risk (CHR), no transition (NTs) and transition (Ts).

| | Controls | CHR | CHR-NTs | CHR-Ts |
|---|---|---|---|---|
| **n Subjects** | 36 | 120 | 96 | 24 |
| **Age** | 24.00 (4.48) | 22.48 (4.61) | 22.71 (4.86) | 24.54 (3.34) |
| **Male** | 20 | 57 | 45 | 12 |
| **Female** | 16 | 63 | 51 | 12 |
| ***Scanner*** | | | | |
| 1 | 25 | 45 | 32 | 13 |
| 2 | - | 5 | 5 | - |
| 3 | 9 | 33 | 33 | - |
| 4 | - | 1 | - | 1 |
| 5 | - | 6 | 4 | 2 |
| 6 | - | - | - | - |
| 7 | 2 | 17 | 12 | 5 |
| 8 | - | 13 | 10 | 3 |
| 9 | - | - | - | - |
| ***Ethnicity*** | | | | |
| White | 26 | 87 | 70 | 17 |
| Black | 2 | 14 | 9 | 5 |
| Mixed | 3 | 10 | 9 | 1 |
| Asian | 1 | 4 | 3 | 1 |
| North African | - | 1 | 1 | - |
| Other | - | 4 | 4 | - |

## 3.2. Cross-sectional Analysis

The results for the cross-sectional structural covariance analysis of the differences between controls and CHR subjects show no significant ($p<0.05$) differences (Figure 10C). However, the significant correlations of controls (Figure 10A) and CHR (Figure 10B) that show up are different. First of all, the number of significant correlations is three times greater in CHR than controls, which may indicate a greater interconnection between regions in the CHR brain.

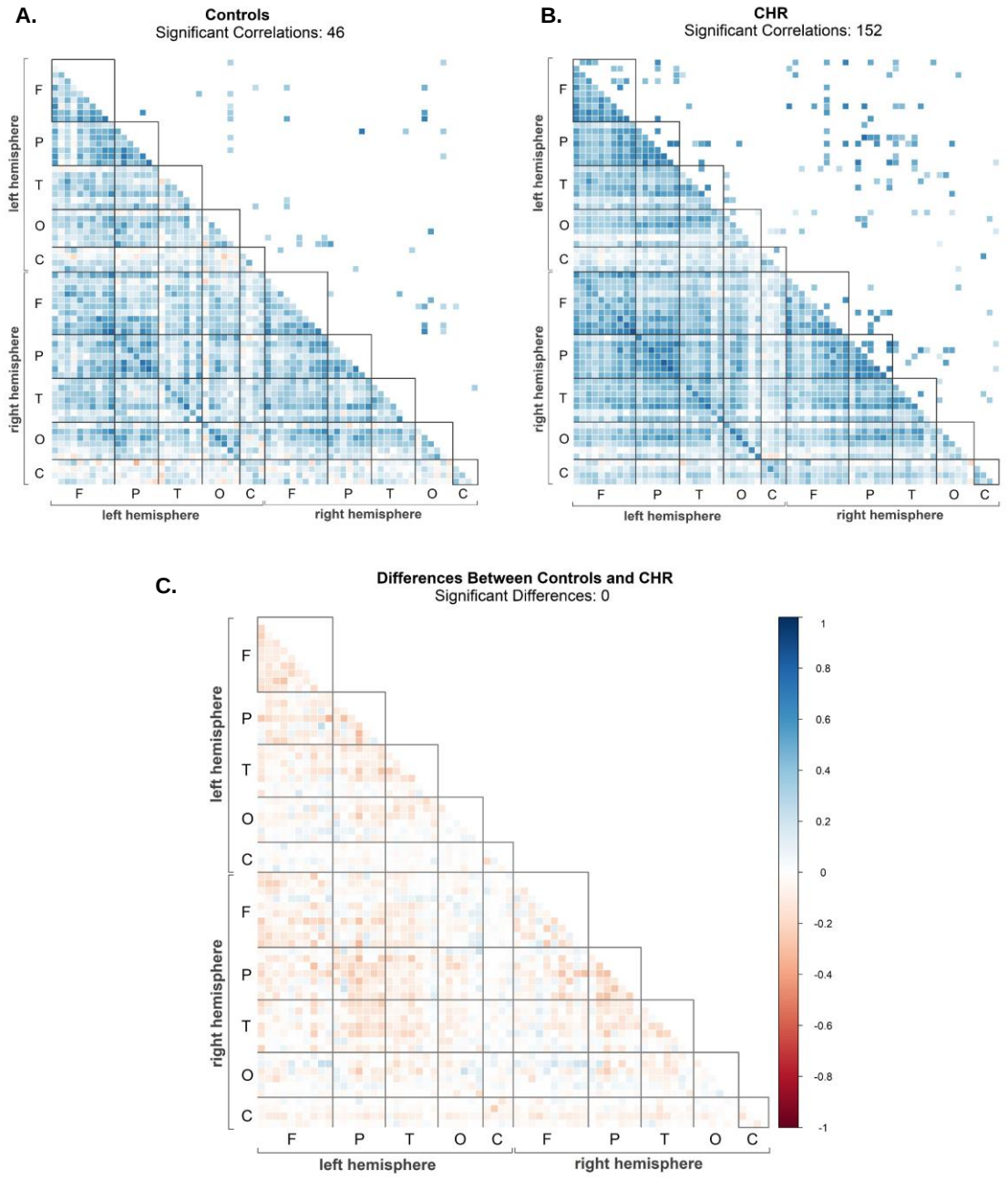


**Figure 10. Structural Covariance Matrices of Significant Correlations and Differences of Controls and CHR subjects.** (A) Significant correlations ($p<0.05$) of the control group. (B) Significant correlations ($p<0.05$) of the CHR group. (C) Significant Differences (FDR-corrected $p<0.05$) between Controls and CHR subjects. Those correlations that are larger in controls are shown in blue, otherwise, in red. In all figures, the lower triangle shows all the correlations or differences, whereas the upper triangle only those that are significant. Abbreviations: clinical-high risk (CHR), frontal lobe (F), parietal lobe (P), temporal lobe (T), occipital lobe (O) and cingulate (C).

Attending to specific regions, for the control group, the region with more significant correlations is left para hippocampal (10 correlations), followed by right medial orbitofrontal, right orbitalis and right para hippocampal (see Appendix B,

Figure B1) - all of them with 6 correlations. However, these regions do not even belong to the significant correlations for the CHR group (see Appendix B, Figure B2). Regarding the regions with more significant correlations in the CHR group (see Appendix B, Figure B2), these are left postcentral (19 correlations), right pars triangularis (15 correlations), right paracentral (13 correlations), left precentral (12 correlations) and right postcentral (12 correlations).

The results for the cross-sectional structural covariance analysis of the differences between controls and CHR subjects show six significant ($p<0.05$) differences (see Table 4 and Figure 11C). These differences are mostly located on the frontal lobe. Except for one significant difference (between left superior frontal and right superior frontal, CHR-NTs>CHR-Ts), the differences are in pairs of regions where there is a greater structural covariance in CHR-Ts compared to CHR-NTs. In Figure 11, this can be seen as all the boxes in the upper triangle are red except for one, which is blue.

**Table 4. Significant differences in the cross-sectional analysis between CHR-NTs and CHR-Ts.** The table shows the two regions that belong to the significant correlation (region 1 and region 2), the value of the significant difference squared (difference: CHR-NTs$^2$ – CHR-Ts$^2$) and the value of the original correlation for both groups (CHR-NTs and CHR-Ts).

| Region 1 | Region 2 | Difference | CHR-NTs | CHR-Ts |
|---|---|---|---|---|
| Left Superior Frontal | Left Caudal Middle Frontal | -0.257 | 0.641 | 0.817 |
| Left Superior Frontal | Right Precentral | -0.309 | 0.550 | 0.782 |
| Left Superior Frontal | Right Superior Frontal | 0.161 | 0.851 | 0.75 |
| Right Inferior Parietal | Left Supramarginal | -0.276 | 0.625 | 0.816 |
| Right Superior Temporal | Right Precentral | -0.355 | 0.498 | 0.777 |
| Right Middle Temporal | Right Banks Superior Temporal Sulcus | -0.364 | 0.522 | 0.773 |

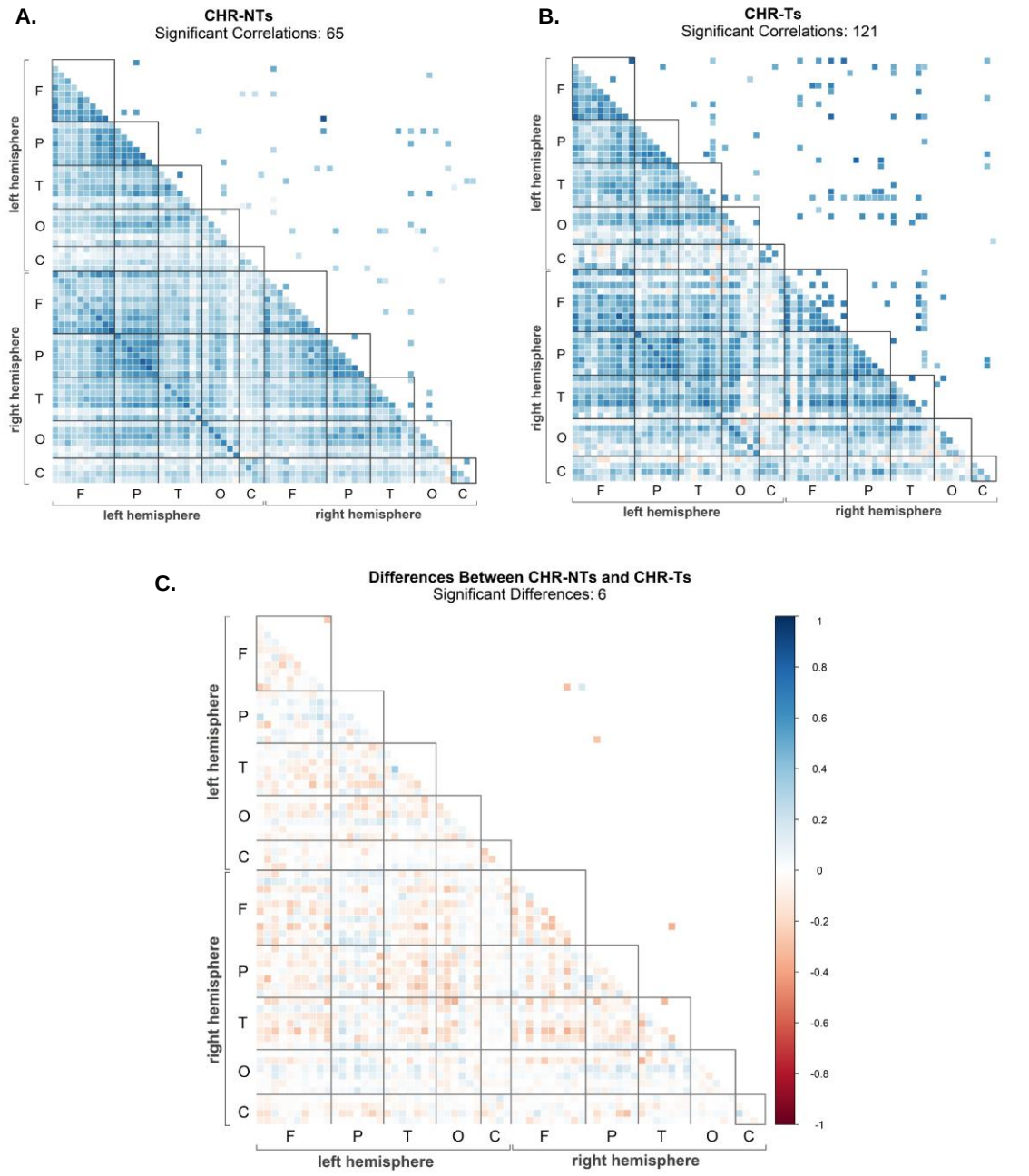


**Figure 11. Structural Covariance Matrices of Significant Correlations and Differences of the CHR-NTs and CHR-Ts subjects.** (A) Significant correlations ($p<0.05$) of the CHR-NTs group. (B) Significant correlations ($p<0.05$) of the CHR-Ts group. (C) Significant Differences (FDR-corrected $p<0.05$) between CHR-NTs and CHR-Ts subjects. Those correlations that are larger in CHR-NTs are shown in blue, otherwise, in red. In all figures, the lower triangle shows all the correlations or differences, whereas the upper triangle only those that are significant. Abbreviations: clinical-high risk no transition (CHR-NTs), clinical-high risk transition (CHR-Ts), frontal lobe (F), parietal lobe (P), temporal lobe (T), occipital lobe (O) and cingulate (C).

### 3.3. Longitudinal Analysis

The results for the longitudinal structural covariance analysis of the differences between controls and CHR subjects show 135 ($p<0.05$) significant differences (Figure 12C). These differences indicate that the brain regions of controls and CHR subjects have a different growth pattern. For instance, two regions that may have a high structural covariance of cortical thickness change, may not have any correlation at all in CHR subjects. This is the case of the pair of regions right isthmus cingulate and right supramarginal that the value of correlations in controls is 0.785 whereas in CHR subjects is -0.002 (see Table 5).

Attending to the significant correlations, both groups show a high number of them (controls: 171, CHR:102). Regarding controls, there is a high structural covariance among almost all regions (see Appendix C, Figure C1), moreover, the most significant correlations (see Appendix C, Table C1) are also strong correlations.

**Table 5. Top significant differences in the longitudinal analysis between Controls and CHR.** The table shows the two regions that belong to the significant correlation (region 1 and region 2), the value of the significant difference squared (difference: Controls2 – CHR2) and the value of the original correlation for both groups (Controls and CHR).

| Region 1 | Region 2 | Difference | Controls | CHR |
|---|---|---|---|---|
| Right Rostral Middle Frontal | Left Pars Opercularis | 0.635 | 0.806 | 0.119 |
| Left Inferior Temporal | Left Supramarginal | 0.633 | 0.847 | 0.289 |
| Right Posterior Cingulate | Right Superior Parietal | 0.624 | 0.866 | 0.354 |
| Right Isthmus Cingulate | Right Supramarginal | 0.617 | 0.785 | -0.002 |
| Left Inferior Temporal | Left Pars Opercularis | 0.616 | 0.82 | 0.238 |
| Right Pars Opercularis | Left Caudal Anterior Cingulate | 0.581 | 0.775 | 0.14 |

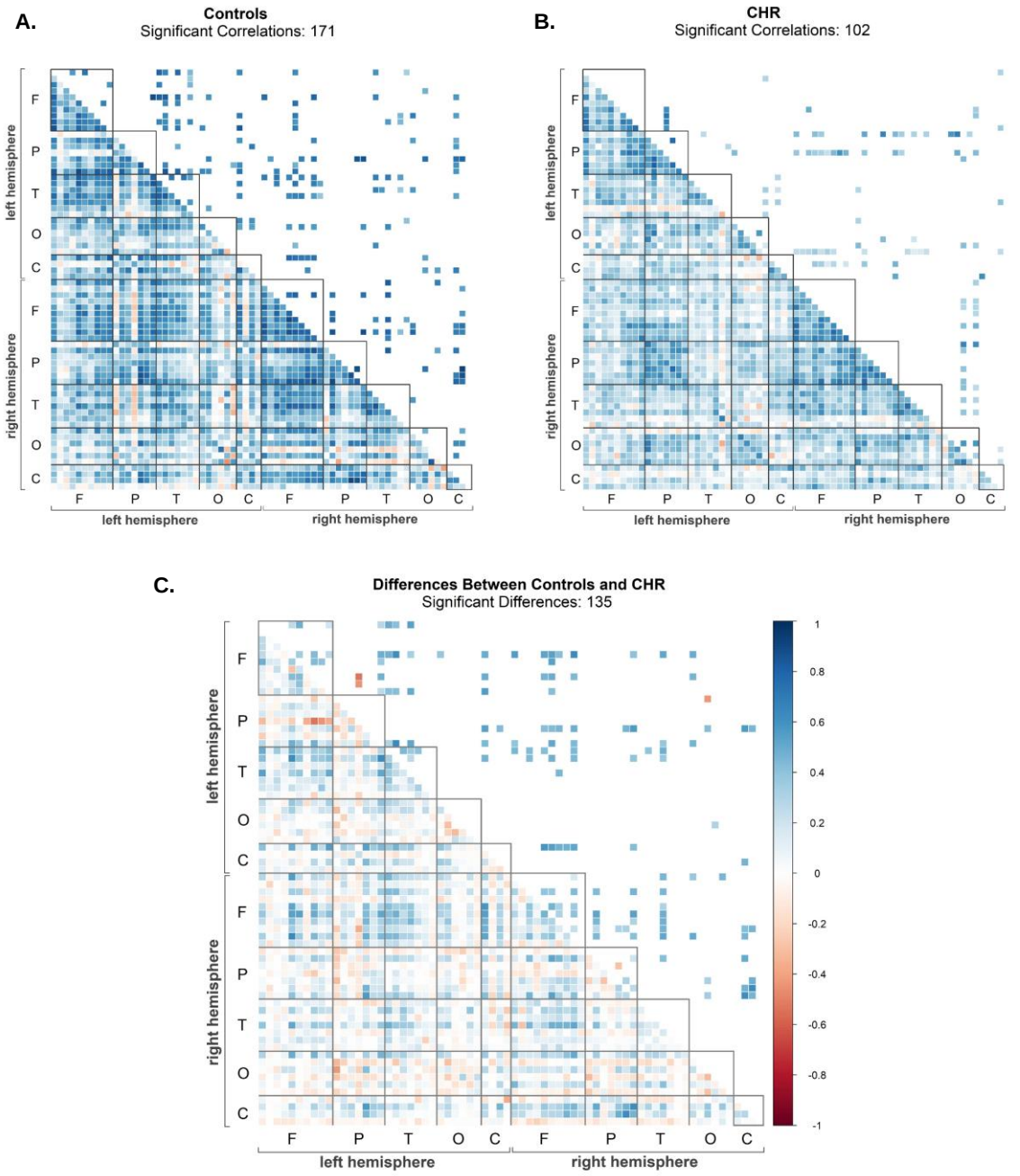


**Figure 12. Longitudinal Structural Covariance Matrices of Significant Correlations and Differences of the Controls and CHR subjects.** (A) Significant correlations of longitudinal change ($p<0.05$) of the controls. (B) Significant correlations of longitudinal change ($p<0.05$) of the CHR group. (C) Significant Differences (FDR-corrected $p<0.05$) between Controls and CHR subjects. Those correlations that are larger in Controls are shown in blue, otherwise, in red. In all figures, the lower triangle shows all the correlations or differences, whereas the upper triangle only those that are significant. Abbreviations: clinical-high risk (CHR), frontal lobe (F), parietal lobe (P), temporal lobe (T), occipital lobe (O) and cingulate (C).

Furthermore, for the control group, the significant correlations involve all the brain lobes (Figure 12A), but the two lobes that are most correlated are frontal and temporal lobes (35 significant correlations). This is not seen for the CHR group (Figure 12B), where the significant correlations are localized in a few regions. The regions with more correlations are left isthmus cingulate (16 correlations), right caudal anterior cingulate (13 correlations), left cuneus (11 correlations), left transverse temporal (9 correlations), right cuneus (9 correlations) and right perical carine (9 correlations). Moreover, the most significant correlations (Appendix C, Table C2) are not strong correlations, unlike what can be seen for the controls. All the aforementioned suggest differences in brain development between controls and CHR subjects.

The results for the longitudinal structural covariance analysis of the differences between CHR-NTs and CHR-Ts subjects show 34 ($p<0.05$) significant differences (Figure 13C). All significant differences show a greater structural covariance of cortical thickness change of CHR-Ts subjects. Of these 34 significant differences, 33 show a greater positive structural covariance in CHR-Ts, this is, the value of correlation is more positive in CHR-Ts than CHR-NTs. The exception is the correlation between right para hippocampal and left superior frontal which has a value of -0.751 in CHR-Ts but almost zero for CHR-NTs ($r=0.059$).

Attending to the significant correlations of CHR-NTs (Figure 13A) and CHR-Ts (Figure 13B), both show a high number of correlations, however, it can be seen that the location of the significant correlations differs between them. For the CHR-NTs, the regions involved in more correlations are left frontal pole (18 correlations), left pars orbitalis (14 correlations), left middle temporal (13 correlations), left temporal pole (13 correlations) and right temporal pole (12 correlations. As it can be seen, the

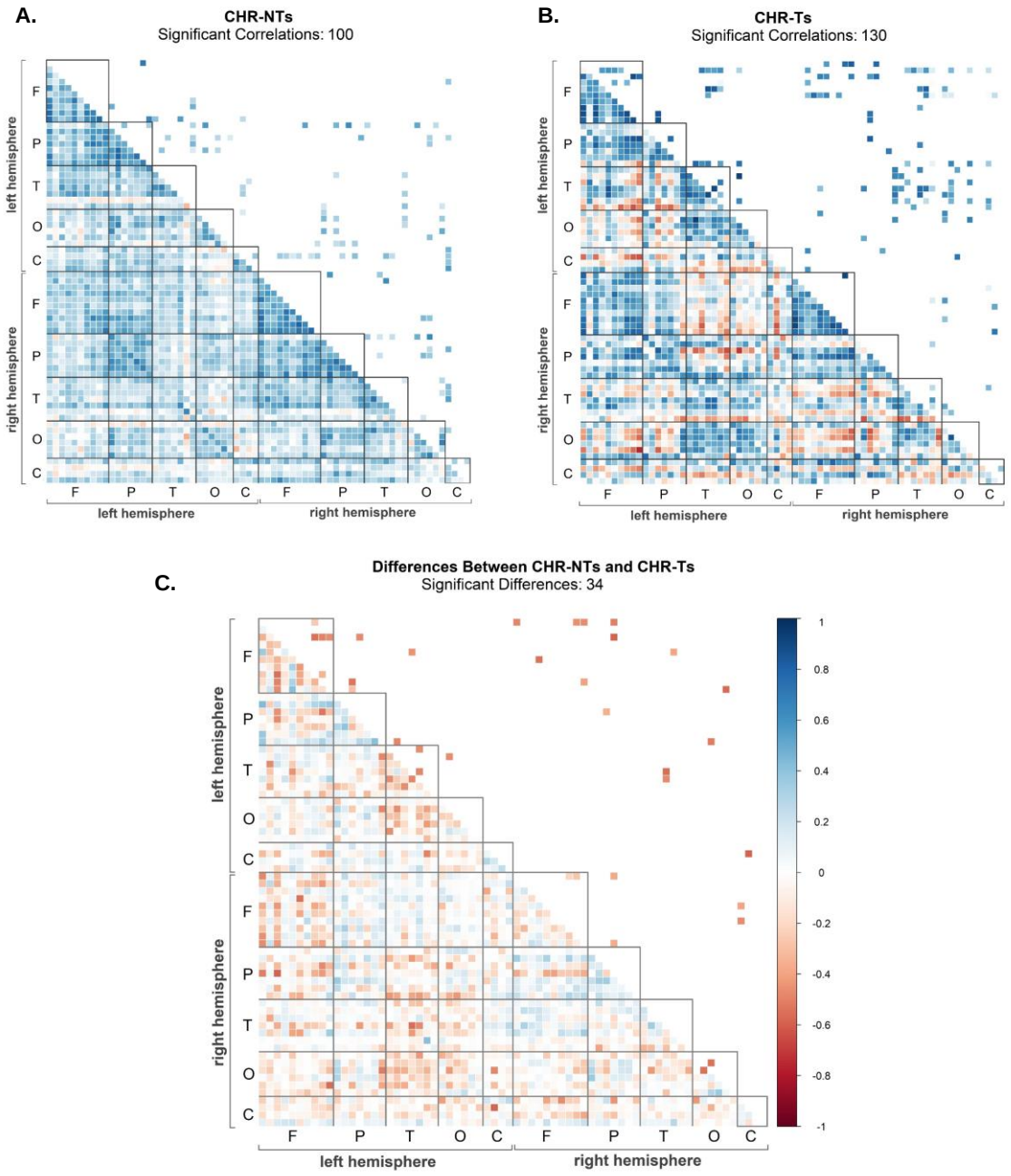


**Figure 13. Longitudinal Structural Covariance Matrices of Significant Correlations and Differences of the CHR-NTs and CHR-Ts subjects.** (A) Significant correlations of longitudinal change ($p<0.05$) of the CHR-NTs group. (B) Significant correlations of longitudinal change ($p<0.05$) of the CHR-Ts group. (C) Significant Differences (FDR-corrected $p<0.05$) between CHR-NTs and CHR-Ts subjects. Those correlations that are larger in CHR-NTs are shown in blue, otherwise, in red. In all figures, the lower triangle shows all the correlations or differences, whereas the upper triangle only those that are significant. Abbreviations: clinical-high risk no transition (CHR-NTs), clinical-high risk transition (CHR-Ts), frontal lobe (F), parietal lobe (P), temporal lobe (T), occipital lobe (O) and cingulate (C).

poles are some of the nodes of these *networks* of significant correlations in CHR-NTs. Moreover, the strength of the most significant correlations varies between 0.2 and 0.6 (see Appendix C, Table C3). Attending to the CHR-Ts group, the first thing that stands out in Figure 13B is the high amount of negative correlations (lower triangle), however, none of those negative correlations are significant. The strength of the significant correlations is high (strong blue in Figure 13B) and the lobes with more correlations can be said to be left frontal, temporal and occipital and right parietal, temporal, occipital and cingulate. The regions with more correlations are left perical carine (18 correlations), left post central (18 correlations), right perical carine (16 correlations), right lingual (14 correlations) and left cuneus (13 correlations).

**Table 6. Top significant differences in the longitudinal analysis between CHR-NTs and CHR-Ts.** The table shows the two regions that belong to the significant correlation (region 1 and region 2), the value of the significant difference squared (difference: CHR-NTs2 – CHR-Ts2) and the value of the original correlation for both groups (CHR-NTs and CHR-Ts).

| Region 1 | Region 2 | Difference | Controls | CHR |
|---|---|---|---|---|
| Right Isthmus Cingulate | Left Isthmus Cingulate | -0.584 | 0.165 | 0.782 |
| Right Post Central | Left Lateral Orbitofrontal | -0.583 | 0.088 | 0.769 |
| Right Para Hippocampal | Left Superior Frontal | -0.561 | 0.059 | -0.751 |
| Right Middle Temporal | Left Middle Temporal | -0.555 | 0.181 | 0.767 |
| Right Medial Orbitofrontal | Left Pars Orbitalis | -0.55 | 0.196 | 0.767 |
| Left Precentral | Left Lateral Orbitofrontal | -0.547 | 0.388 | 0.835 |

# CHAPTER 4. Discussion

In this study, the structural covariance patterns of healthy controls, CHR, CHR-NTs and CHR-Ts have been studied using cortical thickness as a biomarker and using cross-sectional and longitudinal designs. Both designs have helped us study in greater detail the risk of psychosis and its onset. The cross-sectional results found no significant differences between controls and CHR subjects but found 6 significant differences between CHR-NTs and CHR-Ts. As for the longitudinal results, these show a greater number of significant differences between controls and CHR (135 differences) than between CHR-Ts and CHR-NTs (34 differences). Thus, by taking into consideration both designs, the cross-sectional analysis helped us identify the brain connectivity, which is more affected by the transition to psychosis, and the longitudinal design helped us study the difference in growth patterns, which is more affected by being at risk of psychosis than by its onset. Such results evidence the importance of using this method to further study CHR subjects and suggest the disruption of brain connectivity networks, due to the onset of psychosis, and brain developmental process, due to being at risk of psychosis.

Firstly, the results from cross-sectional structural covariance showed differences between CHR-NTs and CHR-Ts among brain regions using correlations of cortical thickness values. These differences are mostly in frontotemporal regions and, except for one correlation, they show increased structural covariance in CHR-Ts (Table 4, Figure 14). Interestingly, these regions have been previously demonstrated to have and abnormal connectivity associated to schizophrenia and to psychosis risk (47). However, no differences were detected when comparing controls to CHR subjects. This suggests that, when looking at structural covariance with a cross-sectional design, we can detect a difference in the transition to psychosis, but we cannot detect a difference between CHR and controls.

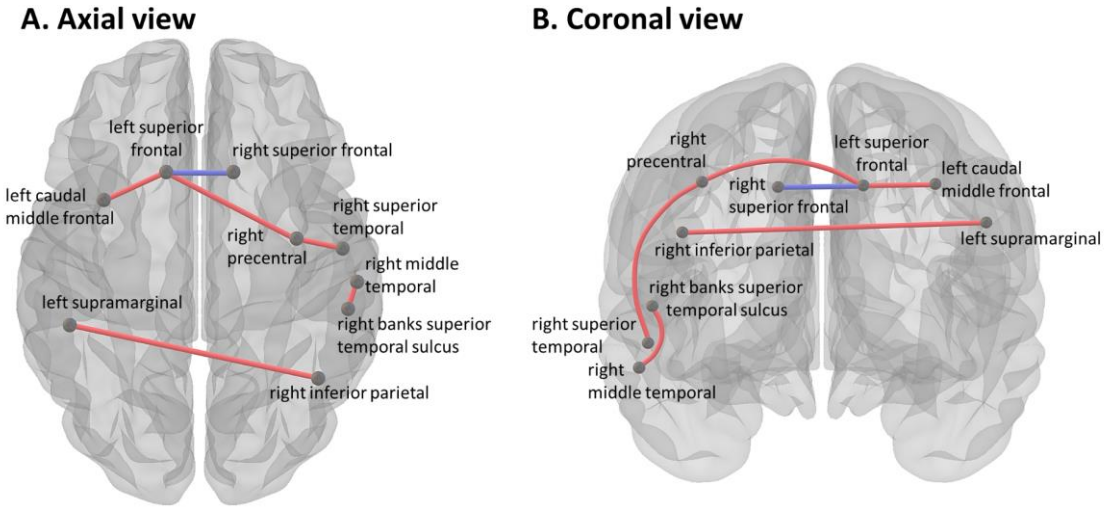


**Figure 14. Significant Differences (FDR corrected, p<0.05) in Structural Covariance patterns between CHR-NTs and CHR-Ts.** Each dot is a brain region (with its label next to it) and each line is a correlation where there was a significant difference between groups. If the line is blue, there is an increased structural covariance between the pair of regions of the CHR-NTs group. Otherwise, if there is greater structural covariance in CHR-Ts than in CHR-NTs for that pair of regions, the line is red. Abbreviations: clinical high-risk no transition (CHR-NTs) and clinical high-risk transition (CHR-Ts).

Furthermore, the significant correlations detected for controls were 46, most of them with a low correlation strength (Figure 10A, r= 0.127 ± 0.148, $r_{min}$= -0.115, $r_{max}$= 0.555). Oppositely, the number of correlations for CHR subjects is high (152 significant correlations) and the strength of the correlations is higher than in controls (r= 0.420 ± 0.134, $r_{min}$= 0.054, $r_{max}$= 0.732), specially between the left hemisphere and the right parieto-temporal regions (Figure 10B). This suggest a greater interconnectivity in CHR subjects (see Appendix B, Figure B2), where almost all brain regions are involved and are strongly connected. Even though our results found no significant differences between controls and CHR subjects, the difference in patterns of significant correlations might suggest what was previously reported regarding differences in connectivity between controls and CHR subjects (47). Looking closer into CHR subjects in order to see if this pattern of strong correlations is common between CHR-NTs and CHT-Ts or if it is unique to one group, the CHT-Ts showed greater correlation between brain regions (r=0.246 ± 0.167, $r_{min}$=-0.21, $r_{max}$=0.652)

compared to those that did not transition to psychosis (r=0.569 ±0.187, $r_{min}$=-0.306, $r_{max}$=0.750). Furthermore, the way the significant correlations were connected was, in case of the CHR-NTs group, in clusters and in a tree form (see Appendix B, Figure B3) but, in the case of the CHR-Ts group, these subjects showed higher connectivity in the linking of significant correlations (see Appendix B, Figure B4). Likewise, previous findings associate a poorer outcome of CHR subjects related to hyper connectivity of within certain brain networks (48,49).

Moreover, the differences between the significant correlations of each group (controls, CHR-NTs and CHR-Ts) of the cross-sectional analyses suggest a change in the wiring of the brain, where specific regions act as hubs of those networks. These hubs change among groups and the correlation strength changes, for instance, controls and CHR subjects show a similar correlation pattern, but the latter has a higher value of correlation. Moreover, significant correlations are not only limited to one lobe, in fact, the number of interhemispheric correlations double the number of interhemispheric correlations for all groups (see Table 7).

**Table 7. Number of significant correlations per hemisphere for each group in the cross-sectional analysis.** The table shows how many correlations were there with both pairs of regions belonging to the left hemisphere (left & left), right hemisphere (right & right) or one region from the left hemisphere and another from the right hemisphere (left & right).

| *Cross-sectional* | *Left & Left* | *Left & Right* | *Right & Right* |
|---|---|---|---|
| Controls | 11 | 23 | 12 |
| CHR | 39 | 77 | 36 |
| CHR-NTs | 14 | 34 | 17 |
| CHR-Ts | 25 | 59 | 37 |

In order to further study the differences between groups, a longitudinal design was used. This design allows the study of the cortical thickness change and how brain regions grow (i.e. the synchronized change between brain regions) among the different groups.

The results of the differences in longitudinal structural covariance between controls and CHR show an increase of differences (from zero in the cross-sectional analysis to 135 in longitudinal design). This shows that there is a difference on how the brain grows in controls compared to CHR subjects. All differences, except for 4 of them, showed a greater structural covariance in controls, meaning that those regions had a greater synchronicity in cortical thickness change (whether it's less or more loss of cortical thickness). Our results here replicate previous studies where it has been reported a decrease/increase of cortical thickness in certain brain regions in CHR compared to controls (50). For instance, one of those brain regions is the cingulate cortex, where there is an increased cortical thickness. Interestingly, Figure 12C shows a number of cingulate regions where there are significant differences between controls and CHR (e.g. right posterior cingulate, left caudal anterior cingulate, etc). Also, as previous studies of first-episode psychosis, our results find many differences in the frontal regions, where it is reported there is a greater loss of cortical thickness in CHR subjects (51). Regions that are said to be impaired in CHR and that are involved in the executive network (52). Furthermore, the matrices of significant correlations of controls (Figure 12A) and CHR (Figure 12B) show that the former group ($r = 0.649 \pm 0.117$, $r_{min}=0.334$, $r_{max}=0.913$) has a higher number of strong significant correlations than the latter ($r = 0.379 \pm 0.138$, $r_{min}= 0.132$, $r_{max}= 0.778$), as well as more numerous (controls 171, CHR 102). This is contrary to what was detected in the cross-sectional analysis, where the CHR subjects had stronger significant correlations. This suggests that controls have a lower connectivity

between brain regions, however these brain regions grow together, which is opposite in CHR subjects.

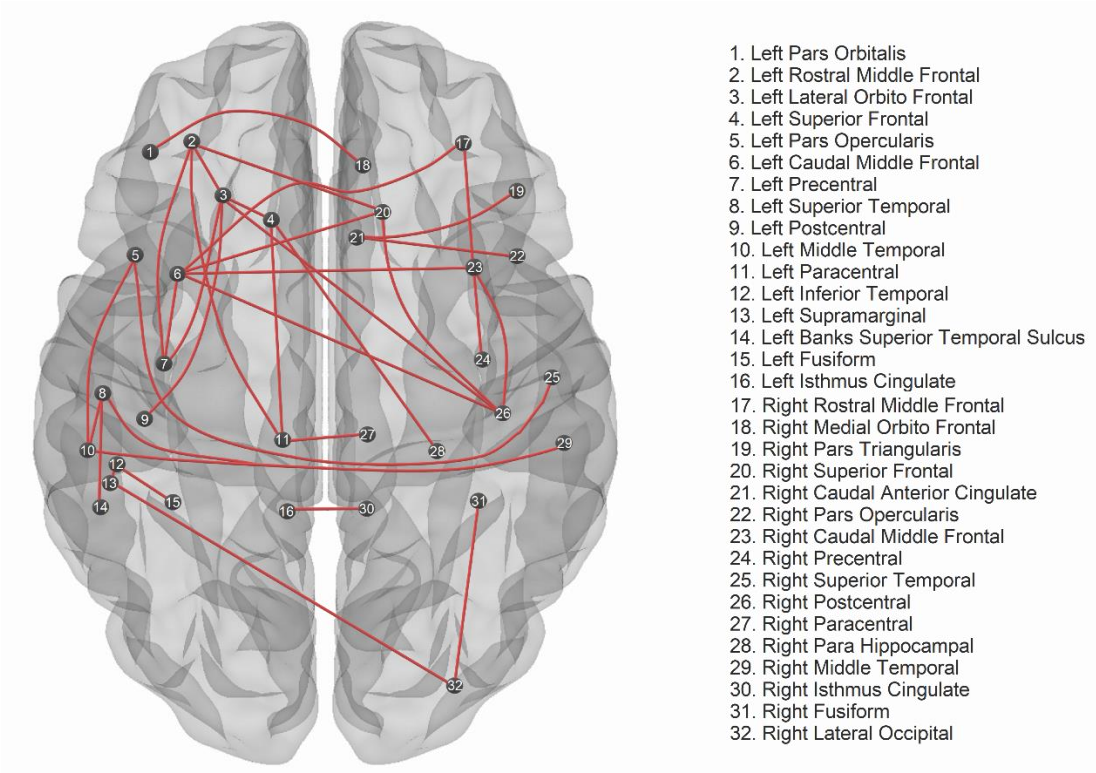


**Figure 15. Significant Differences (FDR corrected, p<0.05) in Longitudinal Structural Covariance patterns between CHR-NTs and CHR-Ts.** Each dot is a brain region (with a number inside which corresponds to the legend) and each line is a correlation where there was a significant difference between groups. If the line is red, there is an increased longitudinal structural covariance between the pair of regions of the CHR-Ts group. Otherwise, the line is blue, but there are no blue lines as there are no correlations where the CHR-NTs group have a stronger value. Abbreviations: clinical high-risk no transition (CHR-NTs) and clinical high-risk transition (CHR-Ts).

Regarding the results of the longitudinal analysis of CHR-NTs and CHR-Ts, these will be discussed here. The number of differences between these groups is 34 and all of these differences show an increased structural covariance in CHR-Ts over CHR-NTs. Such increase is due to a higher loss of cortical thickness in those pairs of regions in CHR-Ts compared to CHR-NTs, which supports the steeper rate of cortical thinning reported in the literature (17). As in the cross-sectional analysis, many of these differences are in frontal regions (Figure 15). Thus, the patterns of cortical thickness change in the frontal lobe with other lobes or within itself are altered

in CHR-Ts compared to CHR-NTs, with a higher synchronicity of the former cohort. Moreover, the pattern seen in Figure 15 suggests differences in both default mode network and central executive network, which have been previously involved in psychosis and schizophrenia (53-55), suggesting a greater cortical thickness change within those regions in those subjects that have transitioned to psychosis. Interestingly, some of the significant differences are between hemispheres, i.e. left with right middle temporal, left with right isthmus cingulate (Figure 15), this asymmetry between lobes has been previously reported to increase in CHR compared to controls, and to increase even more in CHR-Ts (56,57). Furthermore, the fact that CHR-Ts have a higher structural covariance than CHR-NTs can also be observed in their significant correlation matrices (Figures 13A-B), where the matrix of CHR-Ts ($r= 0.544 \pm 0.205$, $r_{min}=-0.026$, $r_{max}=0.931$) show strong blues compared to the light blues seen in CHR-NTs' matrix($r= 0.368 \pm 0.129$, $r_{min}=0.145$, $r_{max}=0.718$). Furthermore, the number of significant correlations is higher for CHR-Ts (130 compared to 100) but is still lower than controls (171 correlations). However, something to highlight is the number of negative correlations that can be seen in CHR-Ts (lower triangle, Figure 13B), which is not comparable to what is seen in any other correlation matrix. These negative correlations are mostly interlobe rather than intralobe. Thus, suggesting that the brain of CHR-Ts subjects grows or thins by lobes rather than as a whole, as it is seen in CHR-NTs and control subjects. In other words, while some regions undergo cortical thinning others undergo cortical thickening.

This study has some limitations. First of all, the fact that it has a multi-site sample, where different scanners were used. This increases the possible artifacts due to scanner bias. Another limitation is the sample size of the longitudinal sample for the CHR-Ts, where there are only 24 subjects, compared to 96 CHR-NTs. This difference in sample size may influence the results, however, when doing the FDR

correction, the sample size of both groups was included to account for it. Another limitation is the fact of not having functional MRI data, which would be useful to merge the structural connectivity results with functional connectivity ones.

Apart from the limitations mentioned above, this study has also many strengths. First of all, the cross-sectional analysis has a large sample size compared to previous studies. It is one of the few studies that uses structural covariance, but it is the first one to compare controls and CHR, and CHR-NTs and CHR-Ts with both longitudinal and cross-sectional designs. Furthermore, the effect of confounders has been taken into consideration in the cross-sectional analysis by regressing out and by using empirical Bayes methods (comBat). As for the longitudinal analysis, the formula to calculate the annual percentual change takes into consideration the confounders too.

Further research should focus on studying structural covariance networks along with functional networks in CHR subjects. Also, replication of the results is needed in order to establish any conclusion from the results in this study. Maturational changes of structural covariance have been proved to report more significant findings than the results obtained in cross-sectional analyses. Thus, the growth patterns of the brain may play a very important role in the transition to psychosis and in the risk of developing psychosis. However, more studies regarding this topic are needed to analyse if the change in growth patterns is psychosis-related and could be used for prediction or if this growth patterns become altered as an outcome of it, which may be useful to predict treatment response.

Finally, this study has been useful to prove another approach that can differentiate between controls and CHR and between CHR-NTs and CHR-Ts. Our results suggest that structural and developmental alterations appear in CHR group and more accentuate in those who transition to psychosis. In this study we have

studied the differences at group level, not at individual level. Thus, further studies should focus on the differences at individual level and maybe use them as a biomarker to predict the subject's outcome and response to treatment or to prevent the onset of psychosis.

## References

(1) Arciniegas DB. Psychosis. Continuum: Lifelong Learning in Neurology 2015;21(3 Behavioral Neurology and Neuropsychiatry):715.

(2) Fusar-Poli P, Tantardini M, De Simone S, Ramella-Cravaro V, Oliver D, Kingdon J, et al. Deconstructing vulnerability for psychosis: Meta-analysis of environmental risk factors for psychosis in subjects at ultra high-risk. European Psychiatry 2017;40:65-75.

(3) Radua J, Ramella-Cravaro V, Ioannidis JP, Reichenberg A, Phiphopthatsanee N, Amir T, et al. What causes psychosis? An umbrella review of risk and protective factors. World Psychiatry 2018;17(1):49-66.

(4) Bois C, Whalley HC, McIntosh AM, Lawrie SM. Structural magnetic resonance imaging markers of susceptibility and transition to schizophrenia: a review of familial and clinical high risk population studies. Journal of Psychopharmacology 2015;29(2):144-154.

(5) Sheffield JM, Karcher NR, Barch DM. Cognitive deficits in psychotic disorders: a lifespan perspective. Neuropsychol Rev 2018;28(4):509-533.

(6) Yamada Y, Inagawa T, Sueyoshi K, Sugawara N, Ueda N, Omachi Y, et al. Social cognition deficits as a target of early intervention for psychoses: a systematic review. Frontiers in psychiatry 2019;10:333.

(7) Fusar-Poli P, Borgwardt S, Bechdolf A, Addington J, Riecher-Rössler A, Schultze-Lutter F, et al. The psychosis high-risk state: a comprehensive state-of-the-art review. JAMA psychiatry 2013;70(1):107-120.

(8) McIntosh AM, Owens DC, Moorhead WJ, Whalley HC, Stanfield AC, Hall J, et al. Longitudinal volume reductions in people at high genetic risk of schizophrenia as they develop psychosis. Biol Psychiatry 2011;69(10):953-958.

(9) Wood SJ, Yung AR, McGorry PD, Pantelis C. Neuroimaging and treatment evidence for clinical staging in psychotic disorders: from the at-risk mental state to chronic schizophrenia. Biol Psychiatry 2011;70(7):619-625.

(10) Heinze K, Reniers RL, Nelson B, Yung AR, Lin A, Harrison BJ, et al. Discrete alterations of brain network structural covariance in individuals at ultra-high risk for psychosis. Biol Psychiatry 2015;77(11):989-996.

(11) Shenton ME, Dickey CC, Frumin M, McCarley RW. A review of MRI findings in schizophrenia. Schizophr Res 2001;49(1-2):1-52.

(12) Pantelis C, Velakoulis D, McGorry PD, Wood SJ, Suckling J, Phillips LJ, et al. Neuroanatomical abnormalities before and after onset of psychosis: a cross-sectional and longitudinal MRI comparison. The Lancet 2003;361(9354):281-288.

(13) Sun D, Phillips L, Velakoulis D, Yung A, McGorry PD, Wood SJ, et al. Progressive brain structural changes mapped as psychosis develops in at risk individuals. Schizophr Res 2009;108(1-3):85-92.

(14) Ziermans TB, Schothorst PF, Schnack HG, Koolschijn PCM, Kahn RS, van Engeland H, et al. Progressive structural brain changes during development of psychosis. Schizophr Bull 2012;38(3):519-530.

(15) Job DE, Whalley HC, Johnstone EC, Lawrie SM. Grey matter changes over time in high risk subjects developing schizophrenia. Neuroimage 2005;25(4):1023-1030.

(16) Pantelis C, Velakoulis D, Wood SJ, Yücel M, Yung AR, Phillips LJ, et al. Neuroimaging and emerging psychotic disorders: the Melbourne ultra-high risk studies. International Review of Psychiatry 2007;19(4):371-379.

(17) Cannon TD, Chung Y, He G, Sun D, Jacobson A, van Erp TG, et al. Progressive reduction in cortical thickness as psychosis develops: a multisite longitudinal neuroimaging study of youth at elevated clinical risk. Biol Psychiatry 2015;77(2):147-157.

(18) Jung WH, Kim JS, Jang JH, Choi J, Jung MH, Park J, et al. Cortical thickness reduction in individuals at ultra-high-risk for psychosis. Schizophr Bull 2011;37(4):839-849.

(19) Fischl B, Dale AM. Measuring the thickness of the human cerebral cortex from magnetic resonance images. Proceedings of the National Academy of Sciences 2000;97(20):11050-11055.

(20) Chen Z, Deng W, Gong Q, Huang C, Jiang L, Li M, et al. Extensive brain structural network abnormality in first-episode treatment-naive patients with schizophrenia: morphometrical and covariation study. Psychol Med 2014;44(12):2489-2501.

(21) Alexander-Bloch A, Raznahan A, Bullmore E, Giedd J. The convergence of maturational change and structural covariance in human cortical networks. Journal of Neuroscience 2013;33(7):2889-2899.

(22) Alexander-Bloch A, Giedd JN, Bullmore E. Imaging structural co-variance between human brain regions. Nature Reviews Neuroscience 2013;14(5):322-336.

(23) Kelly C, Toro R, Di Martino A, Cox CL, Bellec P, Castellanos FX, et al. A convergent functional architecture of the insula emerges across imaging modalities. Neuroimage 2012;61(4):1129-1142.

(24) Zhou J, Gennatas ED, Kramer JH, Miller BL, Seeley WW. Predicting regional neurodegeneration from the healthy brain functional connectome. Neuron 2012;73(6):1216-1227.

(25) Schmitt JE, Giedd JN, Raznahan A, Neale MC. The genetic contributions to maturational coupling in the human cerebrum: a longitudinal pediatric twin imaging study. Cerebral Cortex 2018;28(9):3184-3191.

(26) Romero-Garcia R, Whitaker KJ, Váša F, Seidlitz J, Shinn M, Fonagy P, et al. Structural covariance networks are coupled to expression of genes enriched in supragranular layers of the human cortex. Neuroimage 2018;171:256-267.

(27) Li X, Pu F, Fan Y, Niu H, Li S, Li D. Age-related changes in brain structural covariance networks. Frontiers in human neuroscience 2013;7:98.

(28) Zielinski BA, Gennatas ED, Zhou J, Seeley WW. Network-level structural covariance in the developing brain. Proceedings of the National Academy of Sciences 2010;107(42):18191-18196.

(29) Rosengard RJ, Makowski C, Chakravarty M, Malla AK, Joober R, Shah JL, et al. Pre-onset sub-threshold psychotic symptoms and cortical organization in the first episode of psychosis. Prog Neuro-Psychopharmacol Biol Psychiatry 2020;100:109879.

(30) Zugman A, Assunção I, Vieira G, Gadelha A, White TP, Oliveira PPM, et al. Structural covariance in schizophrenia and first-episode psychosis: An approach based on graph analysis. J Psychiatr Res 2015;71:89-96.

(31) Saiz-Masvidal C, Soriano-Mas C, Contreras F, Mezquida G, Lobo A, González-Pinto A, et al. S18. STRUCTURAL COVARIANCE PREDICTORS OF CLINICAL IMPROVEMENT AT 2-YEAR FOLLOW-UP IN FIRST-EPISODE PSYCHOSIS. Schizophr Bull 2020;46(Supplement_1):S37.

(32) European Network of National Networks studying Gene-Environment Interactions in Schizophrenia, (EU-GEI). Identifying gene-environment interactions in schizophrenia: contemporary challenges for integrated, large-scale investigations. Schizophr Bull 2014;40(4):729-736.

(33) Yung AR, Yung AR, Pan Yuen H, Mcgorry PD, Phillips LJ, Kelly D, et al. Mapping the onset of psychosis: the comprehensive assessment of at-risk mental states. Australian & New Zealand Journal of Psychiatry 2005;39(11-12):964-971.

(34) First MB, Spitzer RL, Gibbon M, Williams JB. User's guide for the Structured clinical interview for DSM-IV axis I disorders SCID-I: clinician version. : American Psychiatric Pub; 1997.

(35) Mallett R. Sociodemographic schedule. Section of Social Psychiatry, Institute of Psychiatry 1997;183.

(36) Desikan RS, Ségonne F, Fischl B, Quinn BT, Dickerson BC, Blacker D, et al. An automated labeling system for subdividing the human cerebral cortex on MRI scans into gyral based regions of interest. Neuroimage 2006;31(3):968-980.

(37) Gennatas ED, Avants BB, Wolf DH, Satterthwaite TD, Ruparel K, Ciric R, et al. Age-related effects and sex differences in gray matter density, volume, mass, and cortical thickness from childhood to young adulthood. Journal of Neuroscience 2017;37(20):5065-5073.

(38) Sowell ER, Peterson BS, Kan E, Woods RP, Yoshii J, Bansal R, et al. Sex differences in cortical thickness mapped in 176 healthy individuals between 7 and 87 years of age. Cerebral cortex 2007;17(7):1550-1560.

(39) Fortin J, Parker D, Tunç B, Watanabe T, Elliott MA, Ruparel K, et al. Harmonization of multi-site diffusion tensor imaging data. Neuroimage 2017;161:149-170.

(40) Pourhoseingholi MA, Baghestani AR, Vahedi M. How to control confounding effects by statistical analysis. Gastroenterology and hepatology from bed to bench 2012;5(2):79.

(41) Johnson WE, Li C, Rabinovic A. Adjusting batch effects in microarray expression data using empirical Bayes methods. Biostatistics 2007;8(1):118-127.

(42) Sternberg RJ, Sternberg RJ. Handbook of human intelligence. : CUP Archive; 1982.

(43) Ankney CD. Sex differences in relative brain size: The mismeasure of woman, too? Intelligence 1992;16(3-4):329-336.

(44) Ritchie SJ, Cox SR, Shen X, Lombardo MV, Reus LM, Alloza C, et al. Sex differences in the adult human brain: evidence from 5216 UK Biobank participants. Cerebral Cortex 2018;28(8):2959-2975.

(45) Rushton JP, Ankney CD. Brain size and cognitive ability: Correlations with age, sex, social class, and race. Psychon Bull Rev 1996;3(1):21-36.

(46) Pol HEH, Schnack HG, Mandl RC, van Haren NE, Koning H, Collins DL, et al. Focal gray matter density changes in schizophrenia. Arch Gen Psychiatry 2001;58(12):1118-1125.

(47) Colibazzi T, Yang Z, Horga G, Yan C, Corcoran CM, Klahr K, et al. Aberrant temporal connectivity in persons at clinical high risk for psychosis. Biological Psychiatry: Cognitive Neuroscience and Neuroimaging 2017;2(8):696-705.

(48) Shim G, Oh JS, Jung WH, Jang JH, Choi C, Kim E, et al. Altered resting-state connectivity in subjects at ultra-high risk for psychosis: an fMRI study. Behavioral and Brain Functions 2010;6(1):58.

(49) Collin G, Nieto-Castanon A, Shenton ME, Pasternak O, Kelly S, Keshavan MS, et al. Brain functional connectivity data enhance prediction of clinical outcome in youth at risk for psychosis. NeuroImage: Clinical 2020;26:102108.

(50) Ding Y, Ou Y, Pan P, Shan X, Chen J, Liu F, et al. Brain structural abnormalities as potential markers for detecting individuals with ultra-high risk for psychosis: A systematic review and meta-analysis. Schizophr Res 2019;209:22-31.

(51) Gutiérrez-Galve L, Chu EM, Leeson VC, Price G, Barnes T, Joyce EM, et al. A longitudinal study of cortical changes and their cognitive correlates in patients followed up after first-episode psychosis. Psychol Med 2015;45(1):205-216.

(52) Seeley WW, Menon V, Schatzberg AF, Keller J, Glover GH, Kenna H, et al. Dissociable intrinsic connectivity networks for salience processing and executive control. Journal of Neuroscience 2007;27(9):2349-2356.

(53) Alloza C, Blesa-Cabez M, Bastin ME, Madole JW, Buchanan CR, Janssen J, et al. Psychotic-like experiences, polygenic risk scores for schizophrenia, and structural properties of the salience, default mode, and central-executive networks in healthy participants from UK Biobank. Translational Psychiatry 2020;10(1):1-13.

(54) Supekar K, Cai W, Krishnadas R, Palaniyappan L, Menon V. Dysregulated brain dynamics in a triple-network saliency model of schizophrenia and its relation to psychosis. Biol Psychiatry 2019;85(1):60-69.

(55) Wotruba D, Michels L, Buechler R, Metzler S, Theodoridou A, Gerstenberg M, et al. Aberrant coupling within and across the default mode, task-positive, and salience network in subjects at risk for psychosis. Schizophr Bull 2014;40(5):1095-1104.

(56) Haller S, Borgwardt SJ, Schindler C, Aston J, Radue EW, Riecher-Rössler A. Can cortical thickness asymmetry analysis contribute to detection of at-risk mental state and first-episode psychosis?: a pilot study. Radiology 2009;250(1):212-221.

(57) Kong X, Mathias SR, Guadalupe T, Glahn DC, Franke B, Crivello F, et al. Mapping cortical brain asymmetry in 17,141 healthy individuals worldwide via the ENIGMA Consortium. Proceedings of the National Academy of Sciences 2018;115(22):E5154-E5163.

# Appendix A. ComBat Results

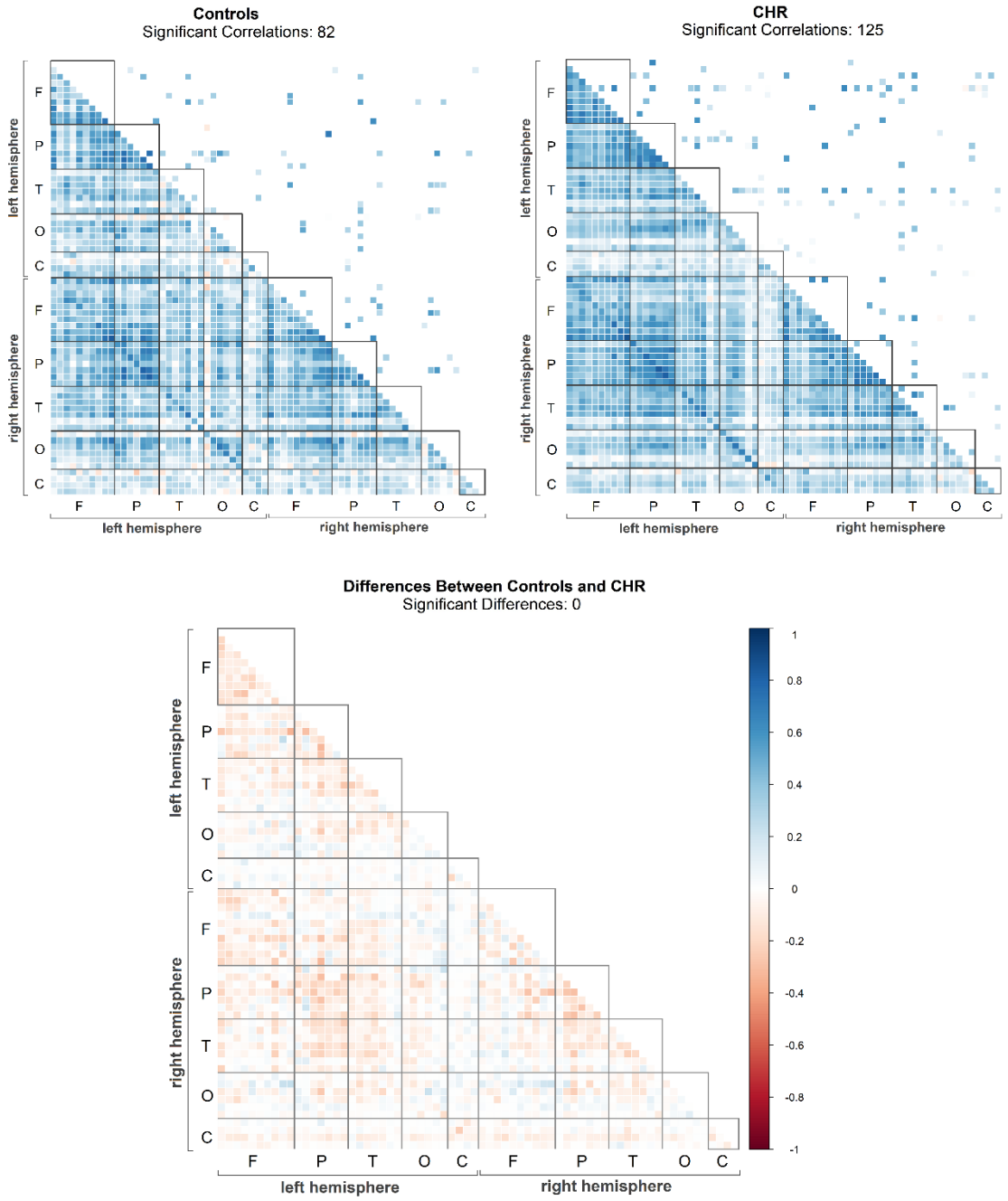


**Figure A1. Structural Covariance Matrices of Significant Correlations and Differences of Controls and CHR subjects (comBat correction).** (A) Significant correlations ($p<0.05$) of the control group. (B) Significant correlations ($p<0.05$) of the CHR group. (C) Significant Differences (FDR-corrected $p<0.05$) between Controls and CHR subjects. Those correlations that are larger in controls are shown in blue, otherwise, in red. In all figures, the lower triangle shows all the correlations or differences, whereas the upper triangle only those that are significant. Abbreviations: clinical-high risk (CHR), frontal lobe (F), parietal lobe (P), temporal lobe (T), occipital lobe (O) and cingulate (C).

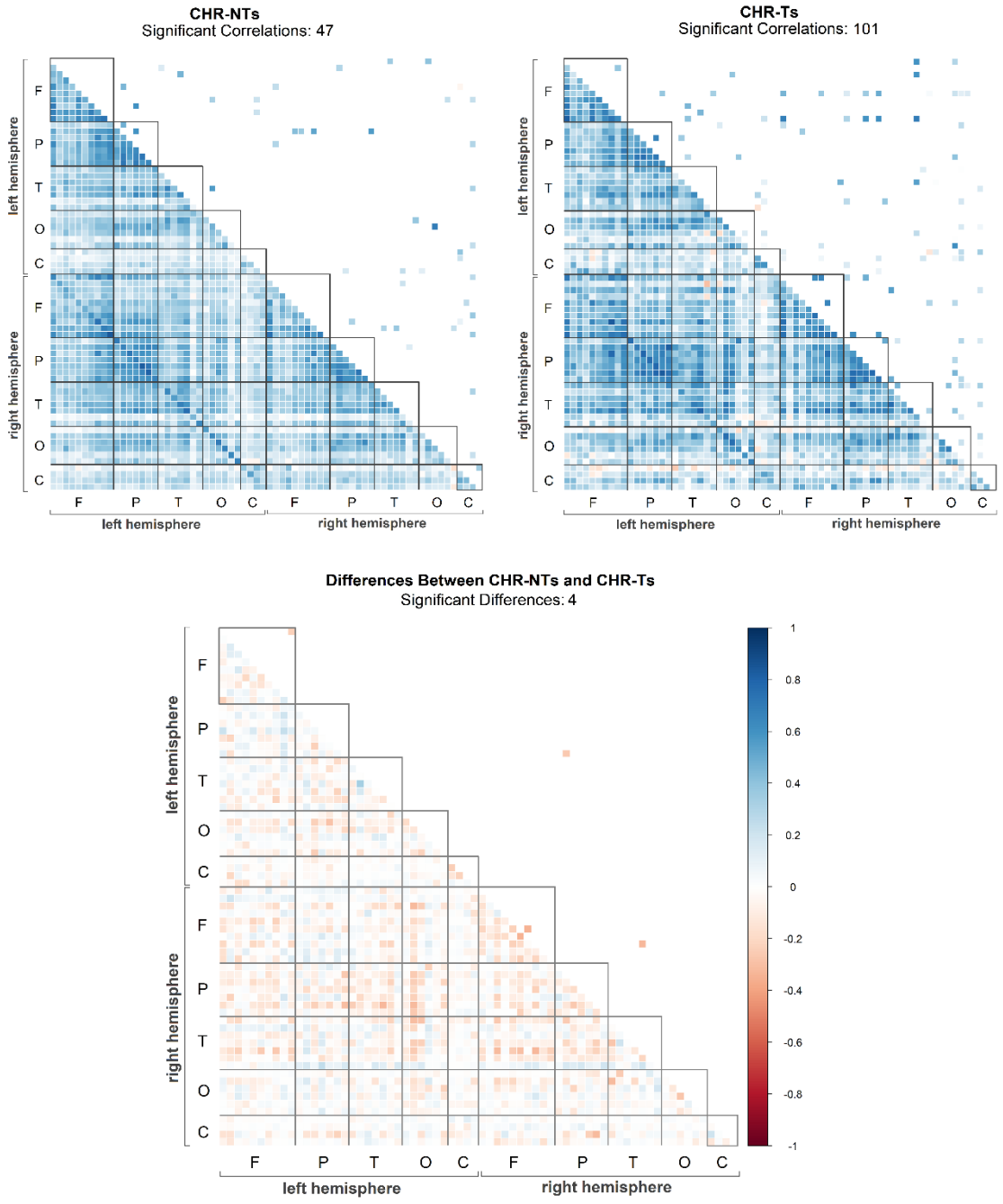


**Figure A2. Structural Covariance Matrices of Significant Correlations and Differences of the CHR-NTs and CHR-Ts subjects (comBat correction).** (A) Significant correlations ($p<0.05$) of the CHR-NTs group. (B) Significant correlations ($p<0.05$) of the CHR-Ts group. (C) Significant Differences (FDR-corrected $p<0.05$) between CHR-NTs and CHR-Ts subjects. Those correlations that are larger in CHR-NTs are shown in blue, otherwise, in red. In all figures, the lower triangle shows all the correlations or differences, whereas the upper triangle only those that are significant. Abbreviations: clinical-high risk no transition (CHR-NTs), clinical-high risk transition (CHR-Ts), frontal lobe (F), parietal lobe (P), temporal lobe (T), occipital lobe (O) and cingulate (C).

# Appendix B: Cross-Sectional Analyses

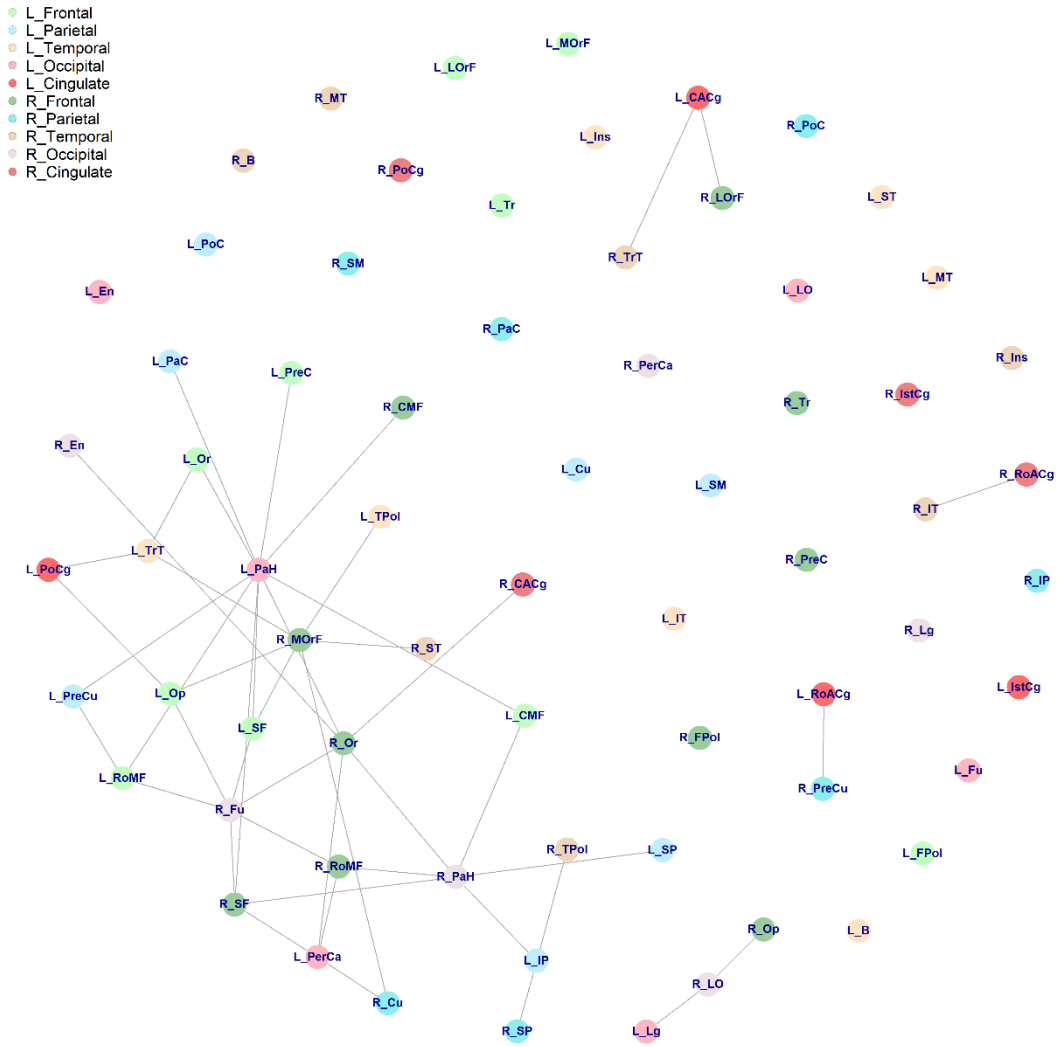


**Figure B1. Alternative representation of the significant correlations for controls.** Each circle is a different brain region (see Appendix D for abbreviations) and each colour is a different lobe. The significant correlations are represented with a line. Those regions that do not belong to a significant correlation are not linked to another region. This representation allows the visualization of hubs and facilitates the understanding of the brain as a network.

**Table B1. Six most significant correlations for controls.**

| Region 1 | Region 2 | P value | Pearson's r |
|---|---|---|---|
| Left Pars Orbitalis | Left Transverse Temporal | 0.004 | 0.081 |
| Left Para Hippocampal | Left Caudal Middle Frontal | 0.006 | -0.031 |
| Left Para Hippocampal | Right Superior Frontal | 0.008 | -0.002 |
| Left Para Hippocampal | Left Superior Frontal | 0.008 | 0.044 |
| Left Para Hippocampal | Left Rostral Middle Frontal | 0.008 | 0.048 |
| Left Temporal Pole | Right Medial Orbitofrontal | 0.010 | -0.115 |

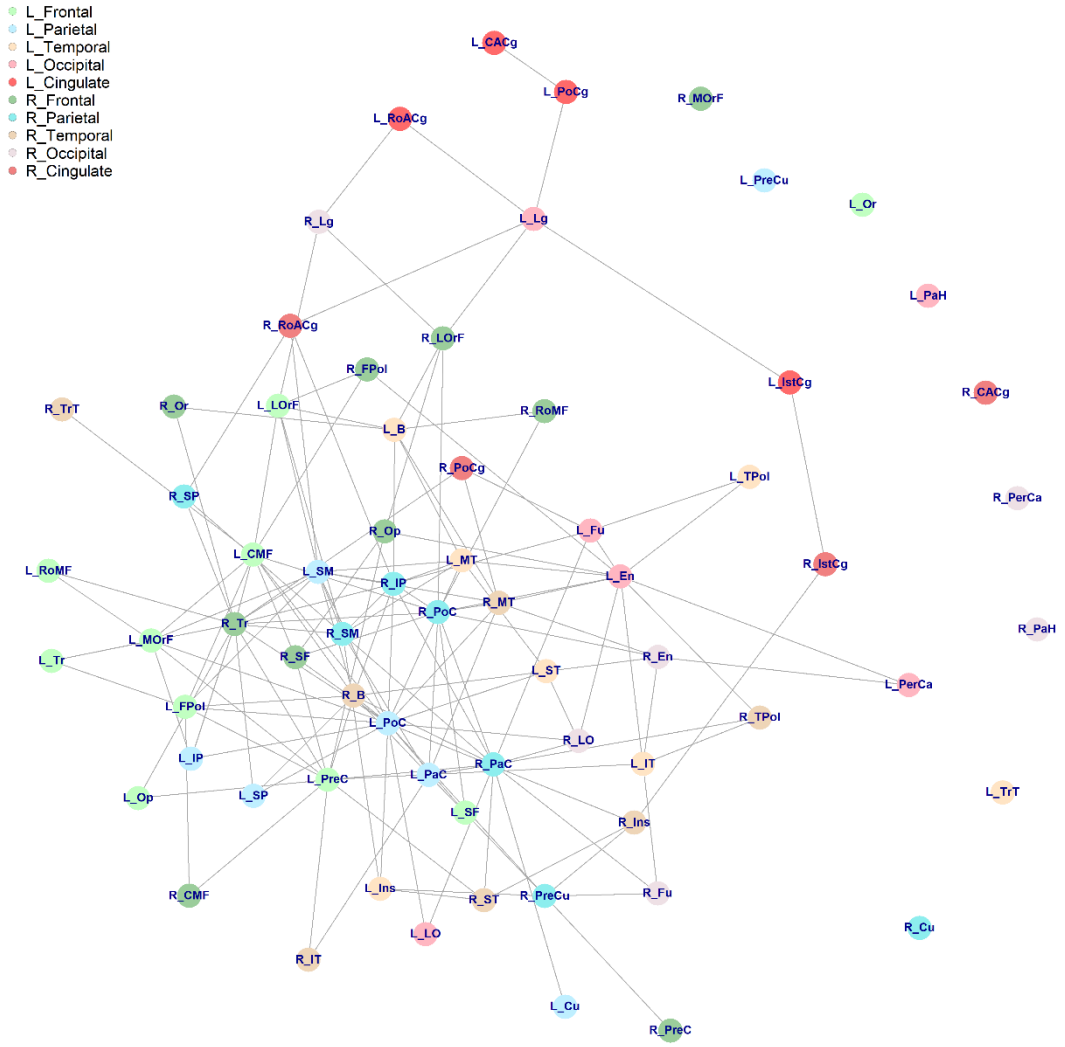


**Figure B2. Alternative representation of the significant correlations for clinical high-risk subjects.** Each circle is a different brain region (see Appendix D for abbreviations) and each colour is a different lobe. The significant correlations are represented with a line. Those regions that do not belong to a significant correlation are not linked to another region. This representation allows the visualization of hubs and facilitates the understanding of the brain as a network.

**Table B2. Six most significant correlations for clinical high-risk subjects.**

| Region 1 | Region 2 | P value | Pearson's r |
|---|---|---|---|
| Left Frontal Pole | Left Precentral | 0.001 | 0.239 |
| Left Caudal Middle Frontal | Right Pars Triangularis | 0.001 | 0.454 |
| Right Pars Triangularis | Right Post Central | 0.001 | 0.529 |
| Left Supramarginal | Right Pars Triangularis | 0.002 | 0.450 |
| Left Post Central | Right Pars Triangularis | 0.002 | 0.510 |
| Left Lingual | Left Rostral Anterior Cingulate | 0.003 | 0.284 |

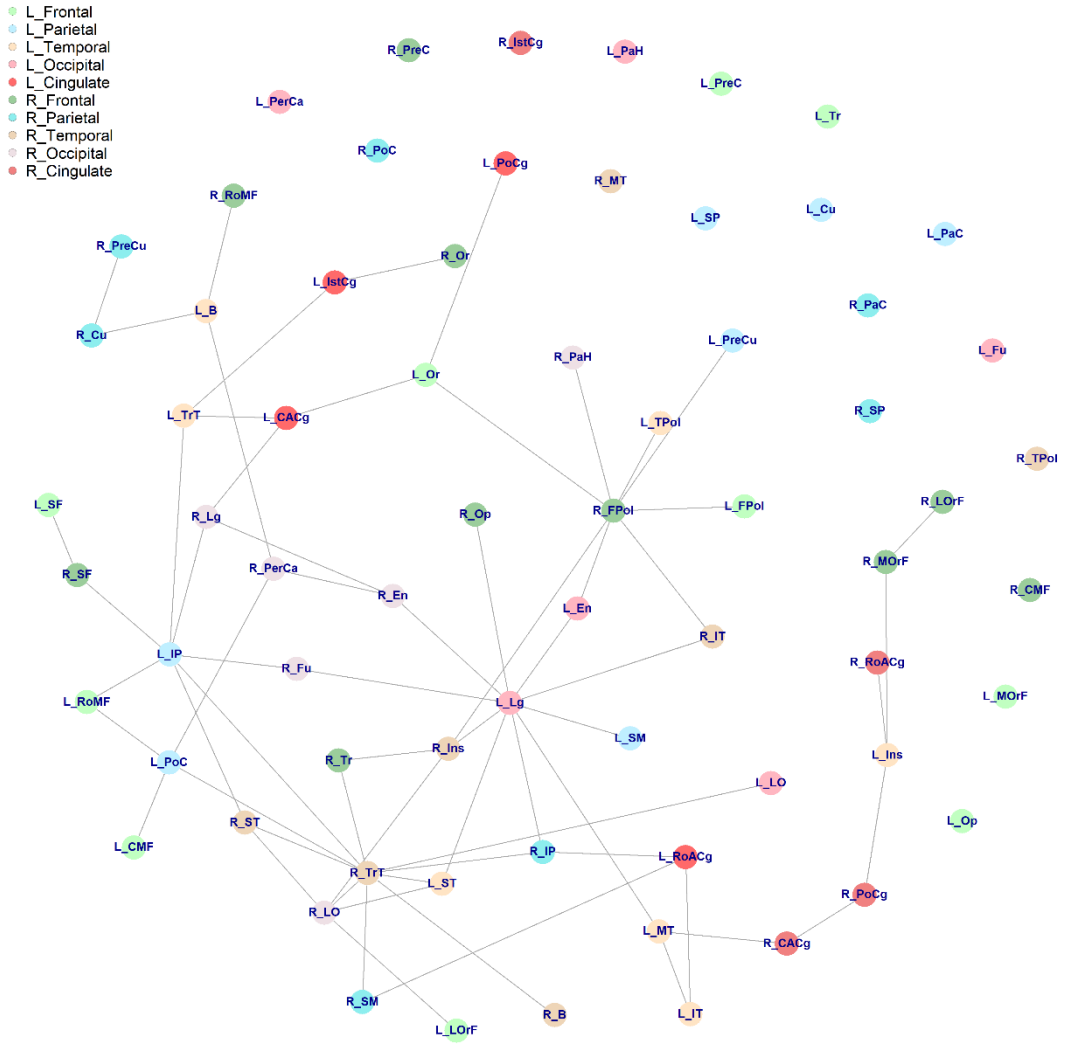


**Figure B3. Alternative representation of the significant correlations for clinical high-risk no transition subjects.** Each circle is a different brain region (see Appendix D for abbreviations)and each colour is a different lobe. The significant correlations are represented with a line. Those regions that do not belong to a significant correlation are not linked to another region. This representation allows the visualization of hubs and facilitates the understanding of the brain as a network.

**Table B3. Six most significant correlations for clinical high-risk no transition subjects.**

| Region 1 | Region 2 | P value | Pearson's r |
|---|---|---|---|
| Left Entorhinal | Left Lingual | 0.001 | -0.246 |
| Right Transverse Temporal | Right Lateral Occipital | 0.001 | -0.125 |
| Left Lingual | Right Pars Opercularis | 0.004 | -0.100 |
| Left Lingual | Right Inferior Temporal | 0.004 | -0.060 |
| Left Inferior Temporal | Left Middle Temporal | 0.006 | 0.293 |
| Left Middle Temporal | Left Lingual | 0.007 | -0.079 |

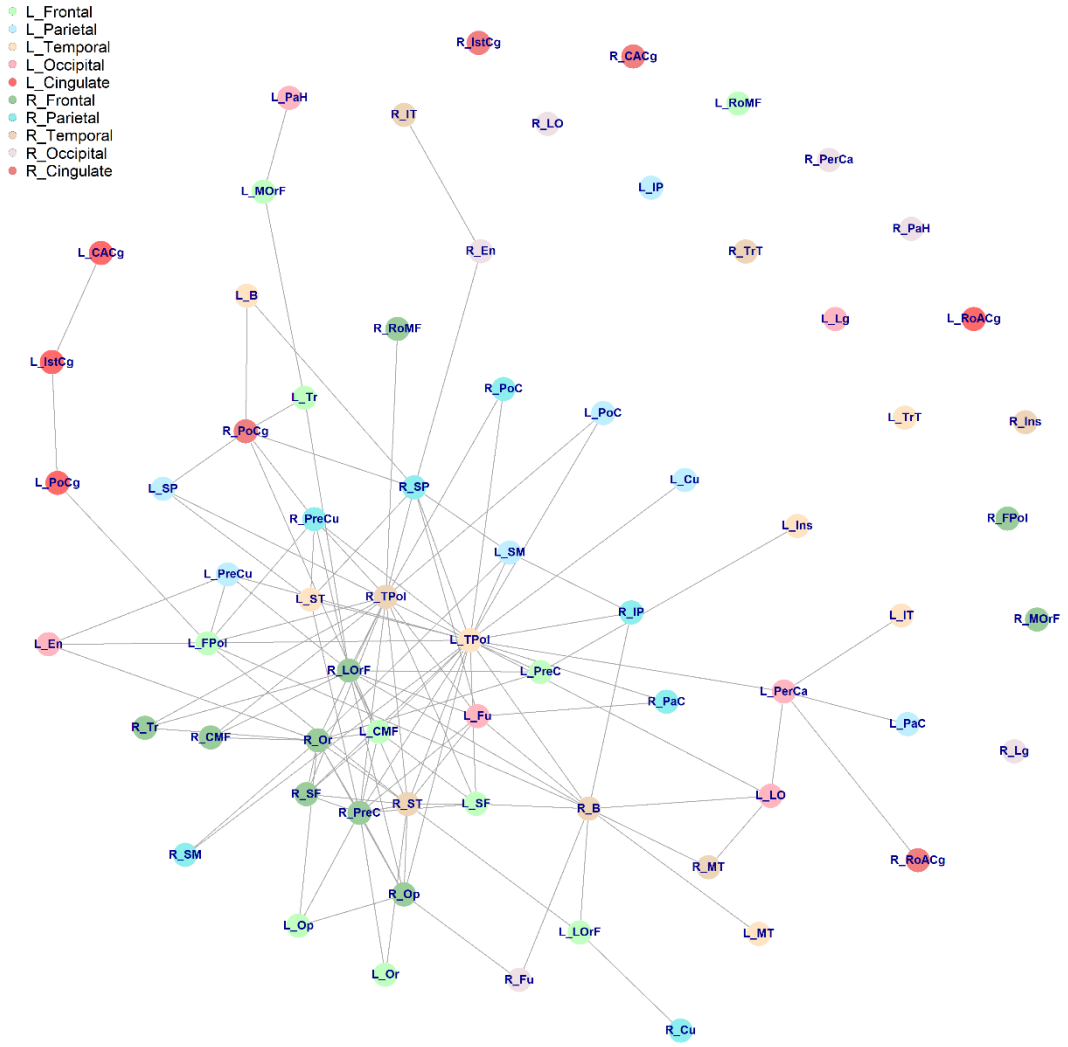


**Figure B4. Alternative representation of the significant correlations for clinical high-risk transition subjects.** Each circle is a different brain region (see Appendix D for abbreviations) and each colour is a different lobe. The significant correlations are represented with a line. Those regions that do not belong to a significant correlation are not linked to another region. This representation allows the visualization of hubs and facilitates the understanding of the brain as a network.

**Table B4. Six most significant correlations for clinical high-risk transition subjects.**

| Region 1 | Region 2 | P value | Pearson's r |
|---|---|---|---|
| Left Precentral | Left Temporal Pole | 0.002 | 0.028 |
| Left Temporal Pole | Right Superior Parietal | 0.002 | 0.089 |
| Left Temporal Pole | Right Paracentral | 0.002 | 0.169 |
| Left Lateral Occipital | Right Banks Superior Temporal Sulcus | 0.002 | 0.274 |
| Right Banks Superior Temporal Sulcus | Right Fusiform | 0.002 | 0.303 |
| Right Pars Orbitalis | Right Precentral | 0.002 | 0.410 |

# Appendix C. Longitudinal Analyses

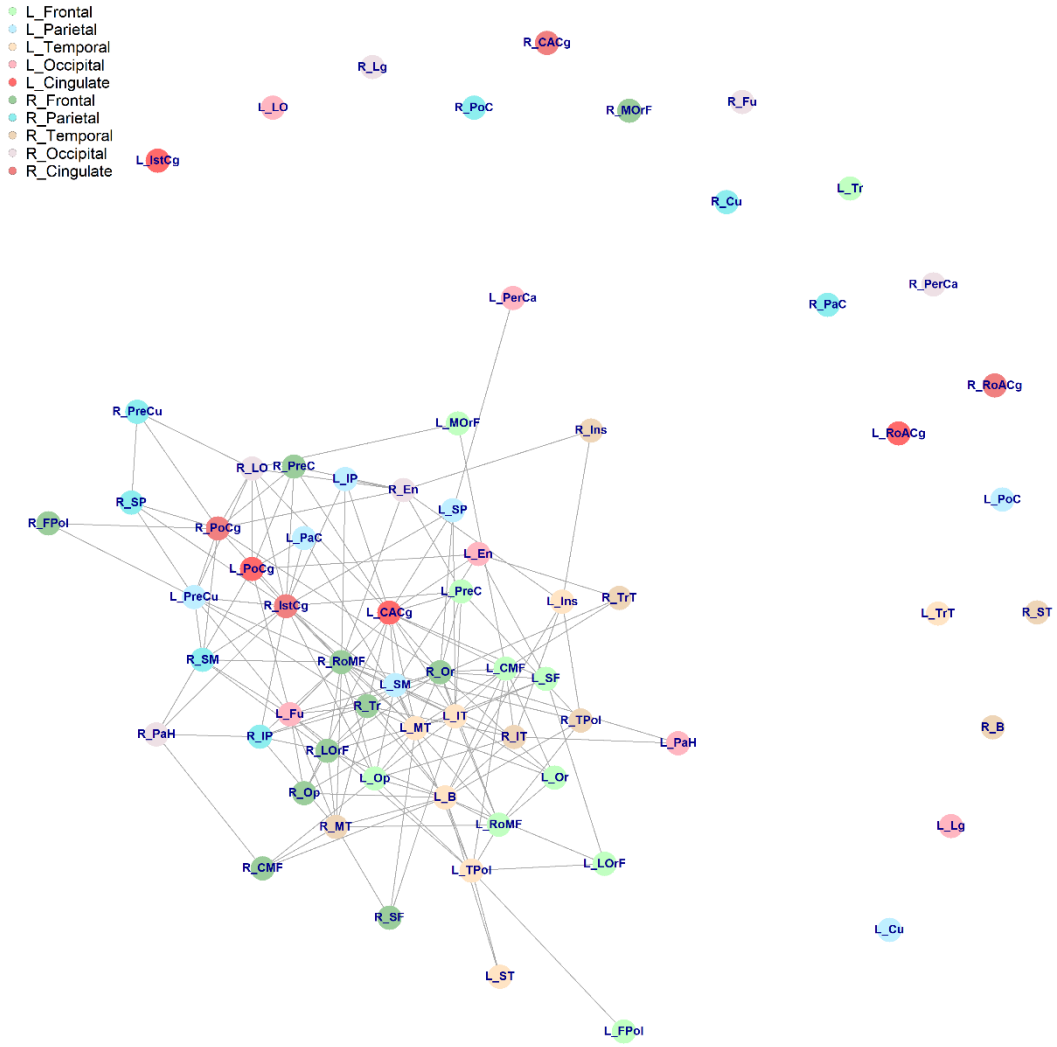


**Figure C1. Alternative representation of the significant longitudinal correlations for controls.** Each circle is a different brain region (see Appendix D for abbreviations) and each colour is a different lobe. The significant correlations are represented with a line. Those regions that do not belong to a significant correlation are not linked to another region. This representation allows the visualization of hubs and facilitates the understanding of the brain as a network.

**Table C1. Six most significant longitudinal correlations for controls.**

| Region 1 | Region 2 | P value | Pearson's r |
|---|---|---|---|
| Right Superior Parietal | Right Posterior Cingulate | 0 | 0.866 |
| Right Precuneus | Right Posterior Cingulate | 0.001 | 0.913 |
| Left Superior Frontal | Left Middle Temporal | 0.001 | 0.718 |
| Left Rostral Middle Frontal | Left Temporal Pole | 0.001 | 0.633 |
| Left Caudal Middle Frontal | Left Middle Temporal | 0.002 | 0.775 |
| Left Precuneus | Right Isthmus Cingulate | 0.002 | 0.75 |

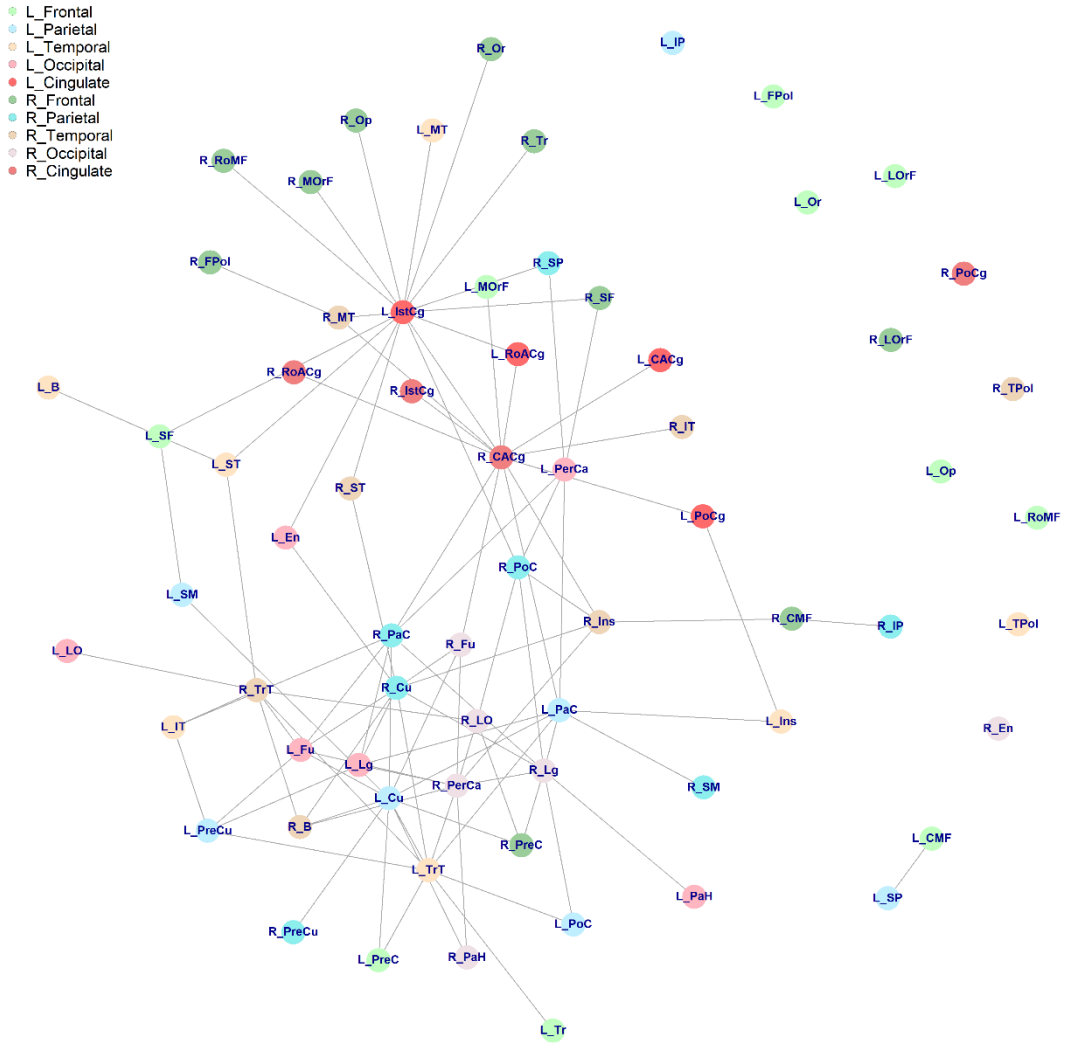


**Figure C2. Alternative representation of the significant longitudinal correlations for clinical high-risk subjects.** Each circle is a different brain region (see Appendix D for abbreviations) and each colour is a different lobe. The significant correlations are represented with a line. Those regions that do not belong to a significant correlation are not linked to another region. This representation allows the visualization of hubs and facilitates the understanding of the brain as a network.

**Table C2. Six most significant longitudinal correlations for clinical high-risk subjects.**

| Region 1 | Region 2 | P value | Pearson's r |
|---|---|---|---|
| Left Perical Carine | Right Lateral Orbitofrontal | 0 | -0.212 |
| Left Perical Carine | Right Pars Orbitalis | 0.001 | -0.042 |
| Left Cuneus | Right Lateral Occipital | 0.002 | 0.21 |
| Left Insula | Left Perical Carine | 0.002 | -0.05 |
| Left Perical Carine | Right Pars Opercularis | 0.002 | -0.074 |
| Left Precentral | Left Postcentral | 0.002 | -0.097 |

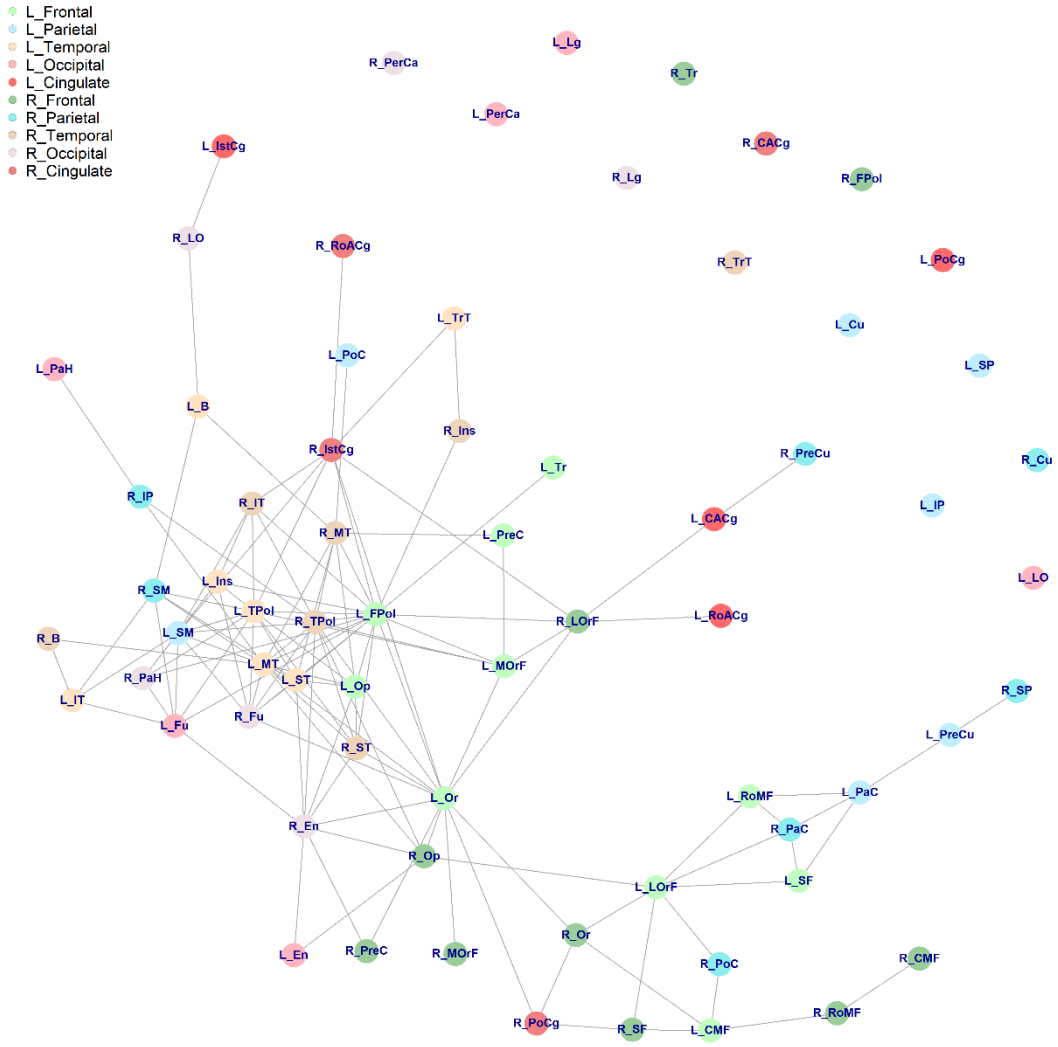


**Figure C3. Alternative representation of the significant longitudinal correlations for clinical high-risk no transition subjects.** Each circle is a different brain region (see Appendix D for abbreviations) and each colour is a different lobe. The significant correlations are represented with a line. Those regions that do not belong to a significant correlation are not linked to another region. This representation allows the visualization of hubs and facilitates the understanding of the brain as a network.

**Table C3. Six most significant longitudinal correlations for clinical high-risk no transition subjects.**

| Region 1 | Region 2 | P value | Pearson's r |
|---|---|---|---|
| Left Rostral Anterior Cingulate | Right Caudal Anterior Cingulate | 0 | 0.654 |
| Right Insula | Right Caudal Anterior Cingulate | 0 | 0.447 |
| Left Isthmus Cingulate | Right Caudal Anterior Cingulate | 0.003 | 0.469 |
| Right Perical Carine | Right Para Hippocampal | 0.005 | 0.341 |
| Right Perical Carine | Left Transverse Temporal | 0.005 | 0.252 |
| Left Cuneus | Left Fusiform | 0.006 | 0.571 |

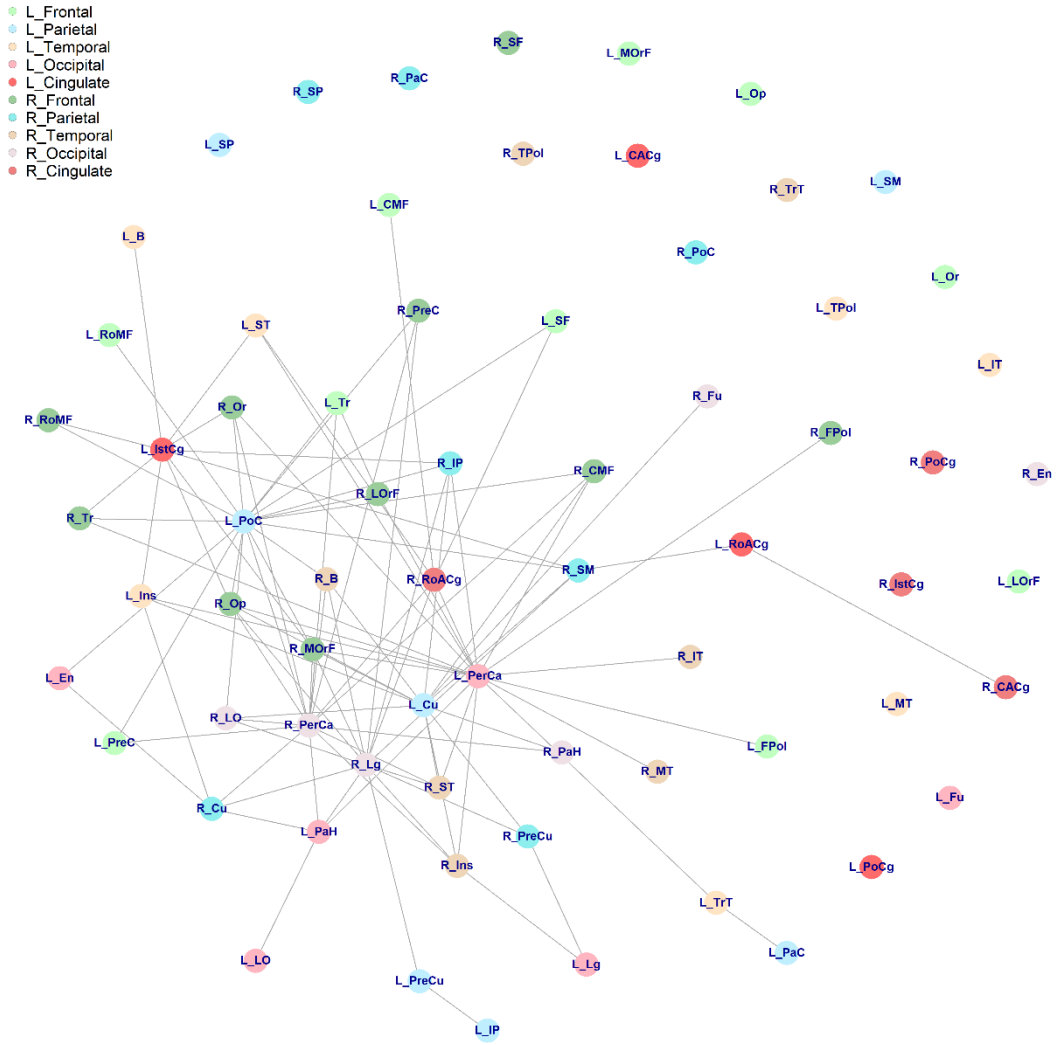


**Figure C4. Alternative representation of the significant correlations for clinical high-risk transition subjects.** Each circle is a different brain region (see Appendix D for abbreviations) and each colour is a different lobe. The significant correlations are represented with a line. Those regions that do not belong to a significant correlation are not linked to another region. This representation allows the visualization of hubs and facilitates the understanding of the brain as a network.

**Table C4. Six most significant correlations for clinical high-risk transition subjects.**

| Region 1 | Region 2 | P value | Pearson's r |
|---|---|---|---|
| Left Middle Temporal | Right Supramarginal | 0 | 0.637 |
| Left Frontal Pole | Left Temporal Pole | 0 | 0.6 |
| Left Frontal Pole | Left Medial Orbitofrontal | 0 | 0.566 |
| Left Frontal Pole | Left Insula | 0.001 | 0.702 |
| Left Frontal Pole | Right Superior Temporal | 0.001 | 0.571 |
| Left Frontal Pole | Right Fusiform | 0.001 | 0.46 |

# Appendix D. Region Abbreviations

**Table D1. Region names and their abbreviations in figures from Appendices B and C.** The abbreviations are preceded by 'L_' for left hemisphere and 'R_' for right hemisphere.

| Region | Abbreviation |
|---|---|
| Left Banks Superior Temporal Sulcus | B |
| Caudal Anterior Cingulate | CACg |
| Caudal Middle Frontal | CMF |
| Cuneus | Cu |
| Entorhinal | En |
| Frontal Pole | FPol |
| Fusiform | Fu |
| Inferior Parietal | IP |
| Inferior Temporal | IT |
| Insula | Ins |
| Isthmus Cingulate | IstCg |
| Lateral Occipital | LO |
| Lateral Orbitofrontal | LOrF |
| Lingual | Lg |
| Medial Orbitofrontal | MOrF |
| Middle Temporal | MT |
| Para Central | PaC |
| Para Hippocampal | PaH |
| Pars Opercularis | Op |
| Pars Orbitalis | Or |
| Pars Triangularis | Tr |
| Perical Carine | PerCa |
| Postcentral | PoC |
| Posterior Cingulate | PoCg |
| Precentral | PreC |
| Precuneus | PreCu |
| Rostral Anterior Cingulate | RoACg |
| Rostral Middle Frontal | RoMF |
| Superior Frontal | SF |
| Superior Parietal | SP |
| Superior Temporal | ST |
| Supramarginal | SM |
| Temporal Pole | TPol |
| Transverse Temporal | TrT |